

Saša Singer¹

Sensitivity of the Heat Transfer Coefficient Calculation

Dedicated to the memory of prof. Mladen Rogina, 1957–2013

Abstract

The purpose of the Liščić/Petrofer probe is to determine the cooling intensity during liquid quenching in laboratory and workshop environments. The surface heat transfer coefficient is calculated by the one-dimensional finite volume method from the smoothed temperature curve, measured at a near-surface point in the probe. Smoothed reference temperature curves for oil and water, based on measurements made by the probe, are used in a series of numerical experiments to investigate the sensitivity of the calculation with respect to various input parameters of the problem, such as: thermal properties of the material, the near-surface thermocouple position, and the diameter of the probe. These results are relevant for other liquid quenchants, at least qualitatively, if not quantitatively. A similar type of analysis is conducted with respect to the variation of numerical simulation parameters in the finite volume method—the choice of space and time steps for problem discretization. When the input curves are sufficiently smooth, the method itself is very reliable.

Keywords: quenching, heat transfer coefficient, surface temperature, core temperature, sensitivity, finite volume method, numerical simulation

AMS Subject classifications: 80A20, 80A23, 65M32

¹Department of Mathematics, Faculty of Science, Bijenička cesta 30, HR–10000 Zagreb, Croatia
(e-mail: singer@math.hr)

Nomenclature

t = time, s

t_{final} = final time for measured temperatures and numerical simulation, s

t_i = discrete time level i in time discretization for numerical simulation, s

τ_i = time step between successive time levels in time discretization, s

τ = finest time step, used at the beginning of the simulation, s

r = radial space coordinate, m (or mm)

D = diameter of the probe, m (or mm)

R = radius of the probe, m (or mm)

d_n = depth of the near-surface thermocouple in the probe, m (or mm)

h = space step in space discretization, m (or mm)

N_{ext} = number of solution extension intervals in space discretization

T = temperature, K or °C

T_n = near-surface temperature, K or °C

T_x = external temperature of the quenchant, K or °C

T_s = surface temperature, K or °C

T_c = core (center) temperature, K or °C

λ = thermal conductivity, W/(m · K)

c = specific heat, J/(kg · K)

ρ = density (mass density), kg/m³

$\gamma = c \times \rho$ = volumetric specific heat, J/(m³ · K)

q = heat flux density, W/m²

q_s = surface heat flux density, W/m²

α = heat transfer coefficient (HTC) at the surface, W/(m² · K)

\vec{n} = unit outer vector perpendicular to the surface

1 Introduction

Quenching probes are standard tools for measuring and evaluating the cooling intensity of various liquid and gas quenchants. They are equipped with one or more thermocouples, that measure and record the temperature curves at selected positions in the probe throughout the whole quenching period of time. The cooling rate, i.e., the time derivative of the temperature at a particular point, can be estimated from the measured cooling curve by approximate numerical differentiation. These two curves (in time) are the basis of all cooling curve tests [1, 2]. Because the calculation of all relevant data is relatively simple, for many years, such tests have been the most useful means for a quick characterization of quenchants, without estimating the actual cooling conditions at the surface—where the heat extraction occurs. In modern times, when the computing power is much greater, standard cooling curve tests are becoming inadequate for accurate simulation and control of the quenching conditions in industrial applications.

The cooling ability of a quenchant is characterized by the heat flux between the hot metal surface and the quenchant. An appropriate model for this heat extraction is Newton's law of cooling [3], combined with Fourier's law of heat conduction

$$q_s = -\lambda \frac{\partial T}{\partial \vec{n}} = \alpha (T_s - T_x), \quad (1)$$

where:

q_s = surface heat flux density, W/m², considered positive when the probe cools,

\vec{n} = unit outer vector perpendicular to the surface,

T_s = surface temperature at a particular point, K or °C,

T_x = external temperature of the quenchant, K or °C, and

α = heat transfer coefficient (HTC) at the surface, W/(m² · K).

The HTC is regarded as the measure of the cooling power of a quenchant, and Eq 1 is used as the boundary condition in numerical simulation of the quenching process, involving solution of the heat conduction equation to predict the hardness of steels (see, for example, [4, 5, 6]).

The reference HTC curves for various quenchants and quenching conditions can be estimated by solving the inverse heat conduction problem (IHCP), where the boundary condition is reconstructed from available input data—one or more measured cooling curves gathered by a particular probe. An overview of different methods for calculating the HTC is given in [1]. However, there are several practical problems common to all methods.

In all experiments, temperatures are measured only at a few points in the probe. It is well known that intensive quenching is not a regular process, and quenching conditions, i.e., the actual HTC values, may be very different at various places on the surface [1]. As a consequence, regardless of the method, all calculated HTCs are some approximations and should be interpreted and used with some caution. The only

way to increase the reliability of estimated HTC's is by repeating the measurements in similar quenching conditions.

The calculation of the HTC from measured temperature curves is an ill-posed problem, meaning that the solution is not well-determined by the input data, and it is very sensitive to measurement errors and small perturbations of the data [3, 7, 8]. Therefore, some form of model transformation and regularization is necessary to obtain a useful solution.

Measured cooling curves are the main input data, and any noise in these curves is very likely to be magnified in the calculated HTC curves. So, the most common initial regularization step is to apply some smoothing procedure to reduce or eliminate the so-called random noise in these data. A general approach to both smoothing and approximation of measured temperatures is described in [2, 9]. Earlier, the effect of different smoothing techniques was analyzed in [10].

Many of the results published in the literature about the HTC are based on relatively small probes, that have only one thermocouple located at the center of the probe (like the ISO 9950 probe). The so-called damping effect frequently results in underestimated peak HTC values. An agreement of the results computed by various methods for the HTC calculation is observed, as in [11], only when the temperature is measured very near or at the surface of the probe. Finally, the HTC values for small probes are much larger than those for larger probes. From the discussion in [2], it follows that the results obtained with small probes have a limited applicability for quenching of much larger pieces in industrial processes.

Apart from that, relatively little is known about the sensitivity of the HTC calculation with respect to all other parameters of the problem, especially when larger probes are used, so that all simple methods for the HTC calculation are not feasible.

The aim of this paper is to fill that gap in the literature and provide some information about the sensitivity of the HTC calculation procedure, and, hopefully, of the HTC itself, with respect to some of the variables involved in the quenching process. The power of numerical simulation is used to perform a number of "experiments" that would be very expensive or even impossible to do in real life, with real probes in actual quenching conditions. To increase the practical value of the results, the initial cooling curves are based on the actual data recorded by the Liščić/Petrofer probe—a large probe designed for characterization of industrial quenching processes [2, 9].

It must be said immediately that this approach is prone to systematic errors in the model and in the software implementation, but it is believed that such errors, if they exist, affect all the experiments in a similar way, so that the results of the sensitivity analysis (with small perturbations) are still reasonably accurate. To verify that, the same type of tests is applied to the actual HTC calculation algorithm.

A brief description of the probe and the HTC calculation is given in the next section, followed by some general sensitivity concerns that influence the design and the scope of all experiments. The results of individual experiments are presented in subsequent sections.

Even though the experiments are based on the data gathered by a particular probe, in only two liquid quenchants, and conducted with a particular algorithm for solving the IHCP, the results presented here should be relevant for other quenchants and other algorithms, that are based on similar principles.

2 Heat transfer coefficient calculation

Complete descriptions of the Liščić/Petrofer probe and the HTC calculation procedure are given in [2, 9], and will be only briefly summarized here.

The probe is a 200 mm long cylinder with the diameter $D = 50$ mm, made of an austenitic nickel–chromium–iron superalloy (Inconel 600², UNS N06600), that does not have phase transformations with the latent heat involved.

The near-surface temperature, denoted by T_n (°C), is measured in time t (s) at the depth $d_n = 1$ mm below the surface, with the highest frequency of 50 measurements per second. Two additional temperatures curves are measured in the probe, one at the depth of 4.5 mm below the surface, and the other one at the center (core). The external quenchant temperature T_x is also known, usually as a constant value at the beginning of the quenching test.

To compensate for the lack of input data, the whole calculation is based on a simplified one-dimensional (1D) model of heat conduction. The probe is considered as a long, radially symmetrical cylinder, with the radius $R = D/2 = 25$ mm, and it is assumed that the temperature T inside the cylinder, for all times $t \geq 0$, depends only on the radial distance $r \in [0, R]$ from the center of the cylinder. The temperature distribution $T = T(r, t)$ inside the cylinder is determined by the one-dimensional heat conduction equation (HCE), written in polar coordinates without the angular component

$$c\rho \frac{\partial T}{\partial t} = \frac{1}{r} \cdot \frac{\partial}{\partial r} \left(r\lambda \frac{\partial T}{\partial r} \right), \quad (2)$$

where c , ρ , and λ are thermal properties of the material:

c = specific heat, J/(kg · K),

ρ = density, kg/m³, and

λ = thermal conductivity, W/(m · K).

As will be shown in one of the sensitivity tests, these properties must be taken as temperature dependent, i.e., as functions of T .

Before each quenching test, the probe is initially heated to about 850 °C, and the initial condition $T(r, 0) = T_0(r)$ at the start of the quenching process is known. Usually, it is assumed that the probe is uniformly heated, so T_0 is constant.

From the radial symmetry assumption, the boundary condition at the center ($r = 0$) must be

$$\frac{\partial T}{\partial r} = 0, \quad (3)$$

and the HTC α at the surface depends only on time t . The boundary condition Eq 1 at the surface ($r = R$) can then be written as

$$q_s = -\lambda \frac{\partial T}{\partial r} = \alpha (T_s - T_x), \quad (4)$$

where $T_s(t) = T(R, t)$ is the (calculated) surface temperature, and T_x is the measured quenchant temperature.

²Inconel alloy 600TM is a trademark of Special Metals Corporation, USA.

The purpose of the probe is to provide further insight into the actual quenching conditions at the surface. To this aim, the HTC is calculated from local information, i.e., from the near-surface temperature T_n , by the so-called solution extension. The remaining two measured curves are used only to verify the computed temperature distribution, but not in the actual HTC calculation.

In this approach, the computed α is very sensitive to the local surface conditions, and this may give somewhat poorer results far away from the surface. On the other hand, it avoids the damping effect deeper in the probe, it is quite fast in practice, and ideally suited for sensitivity tests.

The original temperatures are measured at discrete times, until some final time t_{final} (s), when the probe is sufficiently cool. Before the HTC calculation, the near-surface temperature is smoothed over the whole time range $[0, t_{\text{final}}]$, and this smoothing is the only regularization in the algorithm.

The smoothed near-surface temperature curve, also denoted by T_n , is the main input for the HTC calculation. The HCE (Eq 2) is written as the heat conservation law for the cylinder

$$\int_0^R \left(c\rho \frac{\partial T}{\partial t} \right) (r, t) \cdot r \, r = R \cdot \left(\lambda \frac{\partial T}{\partial r} \right) (R, t) = -R \cdot q_s(t), \quad t \geq 0. \quad (5)$$

The numerical solution of Eq 5 is based on the finite volume method (FVM) [12], because it is easy to incorporate both boundary conditions Eqs 3 and 4 in terms of the heat flux density, and, by doing so, avoid explicit numerical differentiation of temperature at the surface in Eq 4.

The whole computation is performed in four nested loops. From a global perspective, the solution progresses in a series of discrete time levels t_i (s), from the initial level $t_0 = 0$, until the final time is reached.

1. In the outermost loop, the algorithm advances by one time level per step, with the time step $\tau_i = t_i - t_{i-1}$ (s). The solution at the new time level t_i is computed from the solution at the previous level t_{i-1} .
2. At each time level t_i , the surface heat flux density $q_s(t_i)$ is calculated iteratively, until the resulting temperature at the position $R - d_n$ is equal to the smoothed near-surface temperature $T_n(t_i)$. The numerical solution of this equation is done by the Brent–Dekker method [13], and these iterations constitute the middle loop of the algorithm.
3. For each value of the surface heat flux density $q_s(t_i)$, generated by the Brent–Dekker iterations, the remaining two loops compute the temperature distribution over the selected space discretization—finite volumes that determine the space grid, in the whole interval $[0, R]$, by solving the direct HCE problem, written as Eq 5 for all finite volumes. The first inner loop performs simple iterations to adjust all thermal properties to new temperatures at time t_i , until they are stabilized.
4. In each of these iterations, thermal properties at all space-grid points are treated as known. The innermost loop then computes the approximate temperatures at all space-grid points, by solving a tridiagonal linear system of equations.

Step 2 is the key step for solving the IHCP, as it computes the unknown surface heat flux density $q_s(t_i)$ in the boundary condition. Effectively, it performs a solution extension on the interval $[R - d_n, R]$ from the near-surface position to the surface, over the space gap of length d_n . That determines the temperature distribution, including the surface temperature $T_s(t_i)$. After that, the HTC α , as a function of time, is obtained directly from Eq 4, by using the input T_x value.

This method for the solution of the IHCP is especially adapted for large probes with the reference thermocouple located very close to the surface, so that the solution extension toward the surface is performed over a small space gap with respect to the whole radius of the probe. It is not suitable for small probes with a central thermocouple.

3 General sensitivity concerns

Because the HTC calculation is an ill-posed problem, and high sensitivity is expected, before doing any sensitivity tests, every effort has to be made to recognize and possibly eliminate all issues that may influence the validity of the results.

An actual experiment by the probe is subject to many factors that are beyond control, and may affect the results. As an example, the radial symmetry assumption requires strictly vertical immersion of the probe, and vertical agitation of the quenchant. Both assumptions are often violated in practice, resulting in an asymmetrical temperature distribution. For such reasons, sensitivity tests must be conducted in a carefully controlled environment, that is not affected by experimental errors, and they cannot be done by comparing the computed results with measured temperatures. The only reasonable way to do them is by numerical simulation, i.e., by using the same method that is used for the HTC calculation.

The goal of the sensitivity analysis is to determine just how sensitive are various output results with respect to reasonably small perturbations of the input data. These results are used to judge the reliability and numerical stability of the method, and how accurate is the computation of output from input.

However, this should not be confused with the true accuracy of the results. For example, the computed HTC may be nowhere near the true value, which is quite hard to find, anyway. That has to be verified independently—by practical experiments and other computational methods. Once it has been verified that the results are reasonably accurate, then the sensitivity results for the calculation procedure can be extended into some conclusions about the sensitivity of the HTC itself. In that respect, a comparison of the other two measured temperatures with the computed results [2, 9] confirms that the results are satisfactory, within the limits of the simplified 1D model used for calculation.

3.1 General sensitivity of the method

To obtain good results, before the test, all the data has to be prepared carefully, to avoid any potential numerical instabilities in the method, that may be caused by inappropriate data, and the method has to be guarded against such instabilities, as much as possible.

Most of the numerical methods for solving the HCE, including the FVM and the finite difference methods, are very sensitive to the lack of smoothness in the initial and boundary conditions, and in the coefficients of the equation, i.e., in the thermal properties of the material. The cause of that lies in the assumed smoothness of the solution (temperature) that is required to ensure the validity of the equation that is being solved—in this case, Eq 2 or Eq 5. The standard smoothness requirement is that the temperature must be continuously differentiable in time (the so-called C^1 smoothness). It should be noted that this type of sensitivity has nothing to do with the ill-posedness of the HTC calculation.

3.2 Smoothness of input data

The method used for the HTC calculation is extremely sensitive to the smoothness of the near-surface temperature curve $T_n(t)$, for several additional reasons, related to the ill-posedness of the problem. This curve is the only input used in the essential part of the computation to determine the surface heat flux density $q_s(t_i)$, and T_x is used only to calculate $\alpha(t_i)$ from $q_s(t_i)$. The surface conditions are estimated from local information, and $T_n(t_i)$ plays the role of an “internal” reference condition for the solution extension. As the gap is very small, every small wiggle in the input $T_n(t)$ curve is reflected and magnified in the computed $\alpha(t)$ curve. Because there is no other (explicit or implicit) regularization involved in the solution of the IHCP, the near-surface temperature curve $T_n(t)$ must be sufficiently smooth—at least continuously differentiable (C^1 smoothness). Therefore, the smoothing of T_n is an essential part of the data preparation.

It is interesting that the results, including the HTC, are not very sensitive to the choice of the smoothing method, as long as the input curve is sufficiently smooth, and the errors in the approximation of the original measured data are sufficiently small. For example, the reference cooling curves in the next section are prepared by using the cubic spline least-squares approximation [14], which is twice continuously differentiable (C^2 smoothness), while the software that comes with the probe uses exponential C^1 splines [2, 9]. The differences in the HTC are almost negligible, and strictly confined to the high temperature gradients portion of the quenching process.

On the other hand, all local smoothing methods, such as moving averages and local polynomial least-squares approximations, also known as the Savitzky-Golay filters [15], just damp the noise in the data, and the resulting curve may turn out to be insufficiently smooth.

At the beginning of the calculation—at the first time level, it is important to ensure a smooth transition from the initial condition to the boundary or the reference condition, that is used later on. Consequently, to avoid any jumps at the start, the actual value of the initial temperature T_0 is taken from the smoothed temperature curve as $T_0 = T_n(0)$. Because the initial temperature is assumed to be constant over the whole interval $[0, R]$, the heat flux density q (W/m²) between all control volumes, and the initial surface heat flux density $q_s(0)$ must all be equal to zero. Moreover, the same must hold for the first derivative of the temperature, $T'_n(0) = 0$, and this constraint is added in the initial smoothing and approximation of the near-surface temperature curve.

The experience shows that even a small violation of these conditions causes severe

oscillations of the computed solution near the surface for the first few time steps. This may be seen as the numerical instability of the method, but it is just an expected reaction to non-smooth conditions, and can be avoided by proper data preparation.

A similar thing can happen at any time, particularly when intensive cooling begins. All sudden changes in temperature must be C^1 -smooth, at least on the time scale involved in the numerical solution.

3.3 Time advancement and numerical stability

When such oscillations in the solution appear, what happens afterwards, depends on the choice of the time advancement method in the outermost loop of the algorithm. There are three standard choices for the numerical solution of the HCE [12], and they will be described with their usual names, and in terms of numerical time-integration rules (which are used in the FVM implementation).

1. Explicit method (first-point rule for time integration) is stable, i.e., damps these oscillations, only when extremely small time steps are used, and the calculation becomes prohibitively slow.
2. Implicit method (last-point rule for time integration) is unconditionally stable, so large time steps can be used. Any oscillations are relatively quickly damped in a few time steps, but the damage is done in all computed values. Typically, the surface temperature $T_s(t)$ is not monotone, and the jumps are amplified in $q_s(t)$ and $\alpha(t)$ curves. An additional smoothing may be required to remove these artificial oscillations.
3. Crank–Nicolson method (trapezoidal rule for time integration) is, nominally, more accurate than the previous methods. However, it turned out to be very sensitive and unstable—the oscillations always appear and quickly blow up, causing numerical overflow exception.

The implicit method is used in all HTC calculations. Eventual numerical oscillations can be avoided by appropriate smoothing and handling of data. In all the tests reported here, such instabilities have never occurred.

3.4 Smoothness of thermal properties

The values of thermal properties, that appear as coefficients in the HCE, are known only for a small number of temperatures. Before use, these tables have to be converted into functions of temperature over the whole temperature range. Two such functions are needed, one for the so-called volumetric specific heat $\gamma = c\rho$ (J/(m³ · K)), and one for the thermal conductivity λ . Based on the data from [16, 17] for Inconel 600, these functions have been computed by Akima’s piecewise cubic C^1 interpolation [18].

The same can be done by any other form of interpolation (or even approximation) that gives the global C^1 smoothness, such as cubic spline interpolation [19], but not with piecewise linear interpolation.

Even though it is the most commonly used method for converting tables into functions, the piecewise linear interpolation should be avoided in the HTC calculation,

not only for thermal properties, but also for temperatures in time or space. The resulting curve is continuous, but its derivative has jumps at the interpolation nodes, so it is not C^1 -smooth. As a result, such interpolation of thermal properties may drastically increase the number of Brent–Dekker and simple iterations required in steps 2 and 3 of the algorithm.

4 Design and scope of numerical experiments

Numerical experiments for sensitivity tests consist of computing and comparing relevant output results for different values of various input parameters of the problem.

Strictly speaking, the HTC calculation has only two inputs: the smoothed near-surface cooling curve $T_n(t)$, and the (constant) quenchant temperature T_x . In practice, everything else is fixed, as determined by the design of the probe. The main advantage of numerical experiments is that they can go beyond that. Anything that can be considered as an input, or as a parameter of the problem, can be changed and varied, including all numerical parameters in the method.

In this approach to the HTC calculation, the input cooling curve characterizes the whole quenching process in a particular quenchant, and it is obvious that the surface heat flux density and the HTC critically depend on it. But, this dependence is not the target of the tests. Taking different input cooling curves is equivalent to changing quenchants and quenching conditions, and that must be based on the actual data, not on numerical simulation.

Instead of playing with fictive curves representing fictive quenchants, to avoid any misinterpretation of the results, only two cooling curves with fixed corresponding quenchant temperatures are used in all tests. They have been chosen to represent two different liquid quenchants that lie at the opposite ends of quenching intensity:

- mineral oil, non-accelerated and without agitation, with the peak HTC value of about $2,800 \text{ W}/(\text{m}^2 \cdot \text{K})$, and
- water, with the peak HTC value of almost $10,000 \text{ W}/(\text{m}^2 \cdot \text{K})$.

Most other liquid quenchants are somewhere in between these two. A smoothed reference cooling curve has been prepared for each quenchant, based on several measurements by the probe, and then smoothed with all the necessary constraints, as described in the previous section. This means that only two different inputs (in the strict sense) are used for all tests.

With these two inputs, that represent two actual quenchants, the main objective of numerical tests is to find the sensitivity of output with respect to all other parameters of the problem, that cannot be changed easily in practice.

The following five groups of experiments have been conducted by performing a selected set of variations of the corresponding parameter:

1. Thermal properties of the material, used in the HCE to calculate the results.
2. The depth d_n of the near-surface thermocouple, without changing the reference temperatures T_n and T_x , as if the same temperatures $T_n(t)$ are measured at a different position.

3. The diameter D of the probe, with the same depth d_n .
4. The space step h , to test the sensitivity of the calculation (the innermost loop of the algorithm).
5. The time step τ between successive time levels, to test the sensitivity of the calculation (the outermost loop of the algorithm).

The underlying motivation for each group of tests will be discussed along with the results in the next section.

The usual output of the calculation consists of HTC and surface heat flux density curves, together with a number of calculated temperature curves at various points on the radius of the probe. For the purpose of sensitivity analysis, just four of these curves will be considered, and all of them as a function of time t :

- calculated core temperature (for $r = 0$), denoted by T_c ($^{\circ}\text{C}$),
- calculated surface temperature (for $r = R$), denoted by T_s ($^{\circ}\text{C}$),
- calculated HTC α ,
- calculated surface heat flux density q_s .

The core temperature T_c is taken as a representative of what happens far away from the surface, while the last three curves represent the behavior at the surface.

There are several good reasons why the HTC is considered only as a function of time. In gas quenching, which is controllable in time, this is the natural state of affairs. On the other hand, in liquid quenching, the HTC is often taken as a function of the surface temperature T_s . But, from the computational point of view, the HTC is always computed first as a function of time, and then converted into a function of T_s , provided that the surface temperature is monotone decreasing in time. Unfortunately, for some polymer solutions, this is not always the case [2, 9], and requires additional efforts to get the HTC as a function of T_s . Finally, in sensitivity tests, it is much easier to compare the differences in computed HTCs on the fixed time-scale, when only one thing is changed, not two.

The sensitivity is measured in the absolute sense—as the difference between the computed results. To simplify the whole procedure, only one set of output results, computed with standard values of all parameters, will be taken as the reference set for each quenchant (cooling curve). All other results for perturbed data will be compared with these reference results, and only the difference between the reference curve and the “perturbed” curve will be shown.

The results will be presented in a graphical format, in hope that a picture tells a thousand words. The essential information is contained in the scale on the y -axis (that gives the magnitude of the difference, i.e., the result of the perturbation), and in the shape of the difference curve.

4.1 Reference data for oil

The first reference set represents the probe quenched in a low-viscosity plain (non-accelerated) quenching oil, without agitation. The input near-surface temperature curve $T_n(t)$ and the quenchant temperature $T_x = 66^\circ\text{C}$ are shown in left part of Fig. 1 for the whole quenching period of 900 seconds. The calculated temperatures $T_s(t)$ at the surface, and $T_c(t)$ at the core, are also shown in the same figure. These two temperatures are taken as the reference curves in all subsequent tests for oil.

The quenching process is quite slow, and intensive cooling starts relatively late, after about 36 seconds. The right part of Fig. 1 shows all the temperatures during the most intensive part of the quenching period, in the fine time-scale. The same style of dual time-scale presentation will be used through, where appropriate.

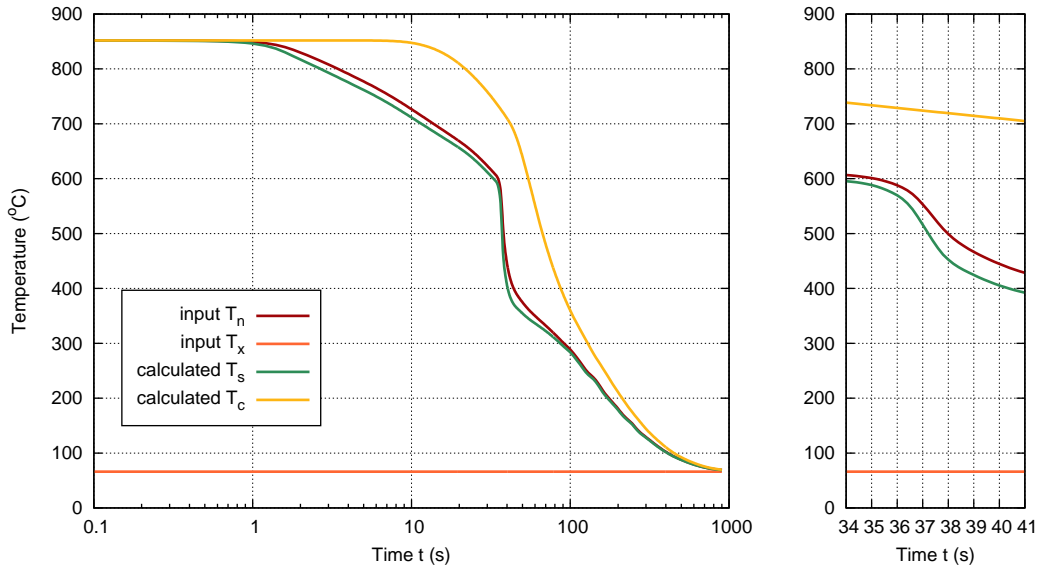


Fig. 1 Oil (reference): input near-surface and quenchant temperatures, and calculated surface and core temperature curves.

The calculated HTC and the surface heat flux density q_s are shown in Figs. 2 and 3, and they are taken as the corresponding reference curves in all tests for oil.

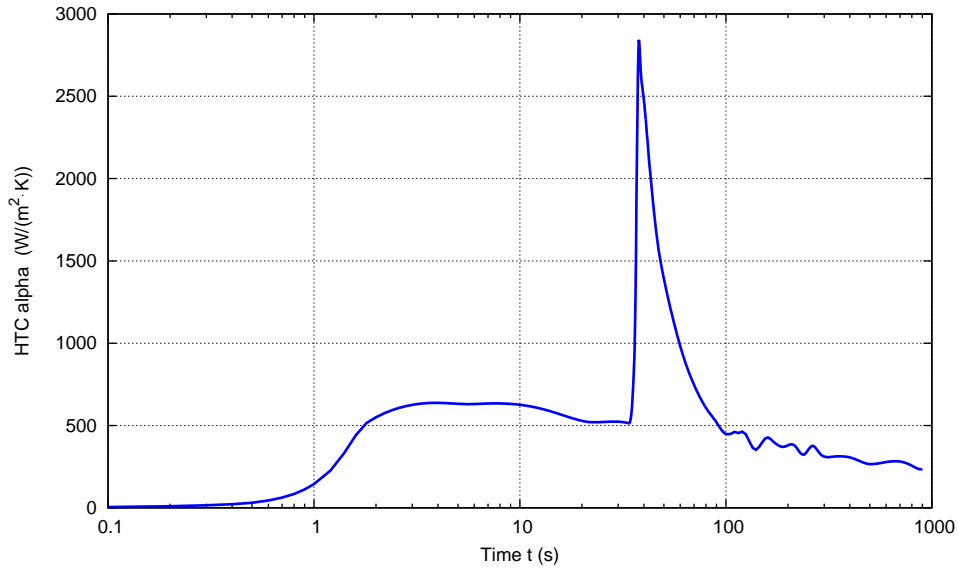


Fig. 2 Oil (reference): calculated HTC as a function of time.

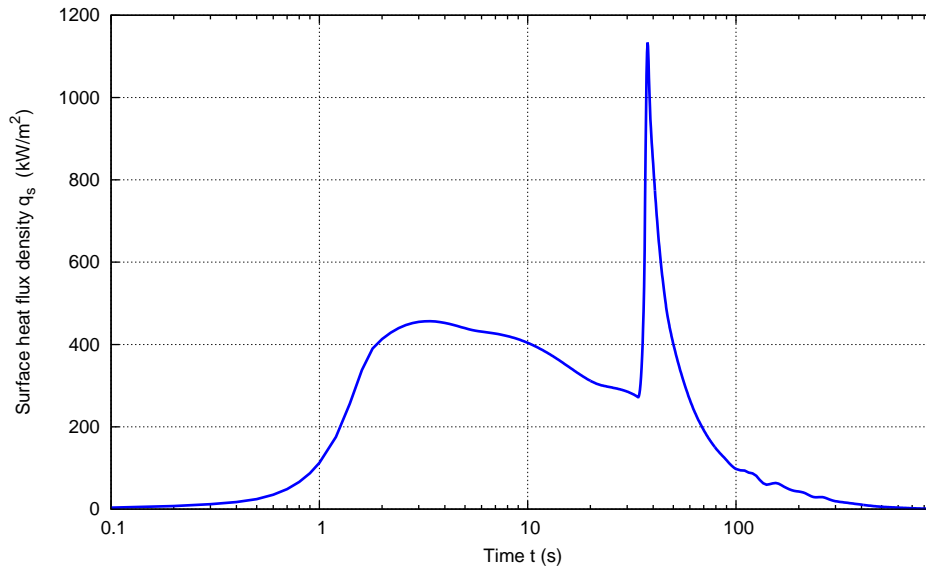


Fig. 3 Oil (reference): calculated surface heat flux density as a function of time.

4.2 Reference data for water

The second reference set represents the probe quenched in water at the temperature $T_x = 38^\circ\text{C}$. The input near-surface temperature curve $T_n(t)$ and T_x are shown in the left part of Fig. 4, together with the calculated surface and core temperatures, $T_s(t)$ and $T_c(t)$ (the reference curves for water), for the whole quenching period of 300 s.

The quenching in water is much quicker, and intensive cooling starts quite soon, after only 10 seconds. Again, the right part of Fig. 4 shows all the temperatures during the most intensive part of the quenching period, in the fine time-scale.

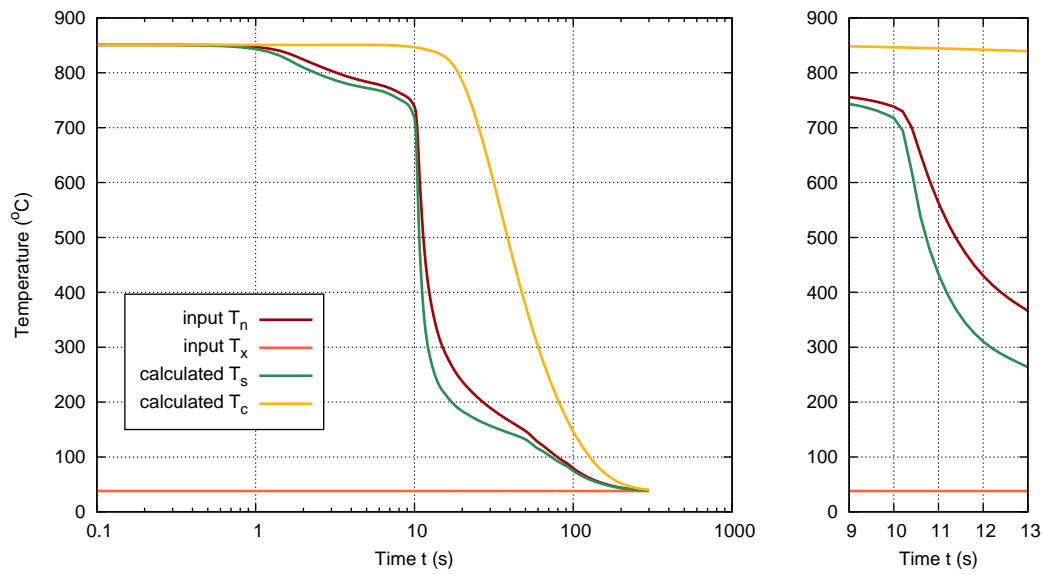


Fig. 4 Water (reference): input near-surface and quenchant temperatures, and calculated surface and core temperature curves.

The calculated HTC and the surface heat flux density q_s are shown in Figs. 5 and 6, and they are taken as the corresponding reference curves in all tests for water.

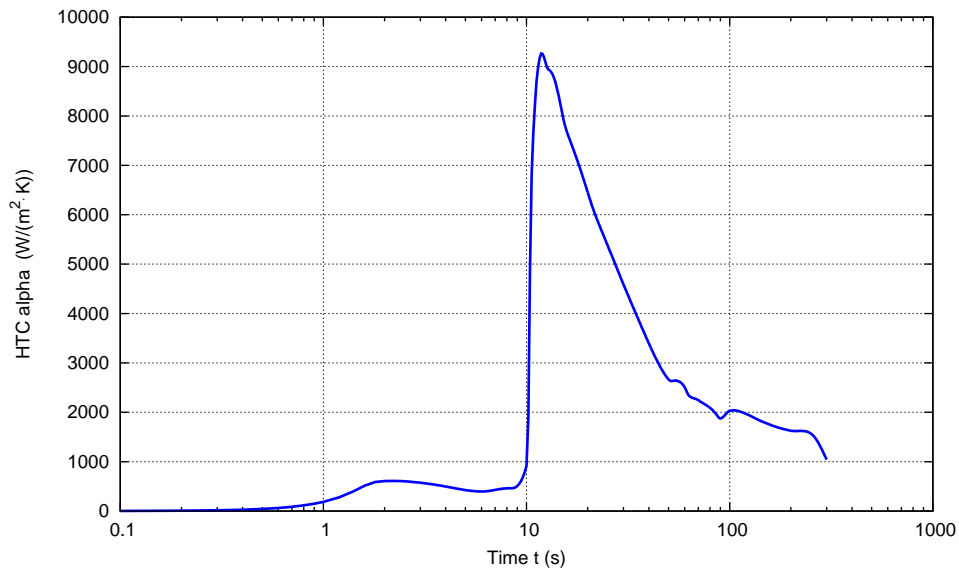


Fig. 5 Water (reference): calculated HTC as a function of time.

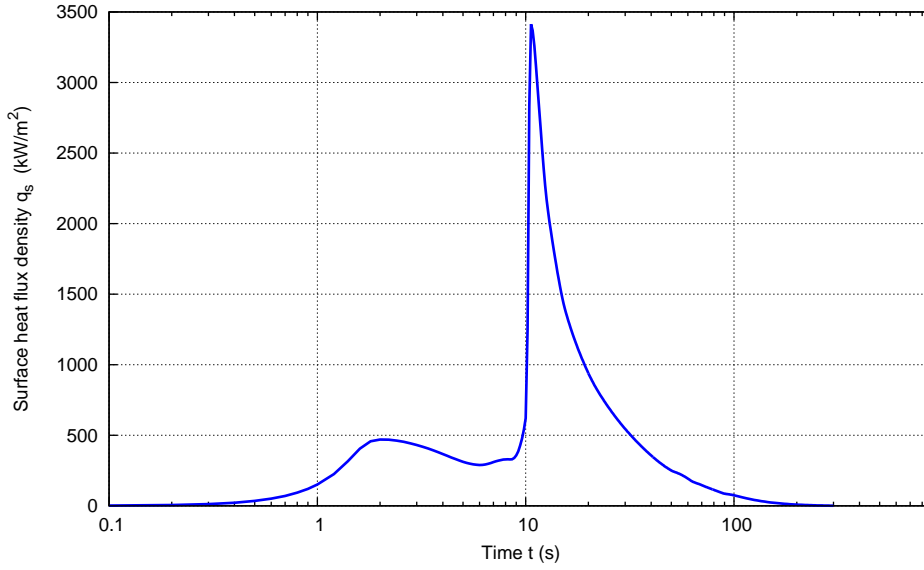


Fig. 6 Water (reference): calculated surface heat flux density as a function of time.

In both HTC curves, shown in Figs. 2 and 5, small waves or wiggles can be seen relatively near the end of the quenching process (in the logarithmic time-scale), starting around 130 seconds for oil, and around 50 seconds for water. They are caused by the actual phenomenon at the surface, when the quenchant layer near the surface becomes sufficiently cool to stop boiling, and only sporadic vapor bubbles are formed, before it turns into the entirely liquid state.

5 Results of sensitivity tests

This sections contains the computed results for all five groups of sensitivity tests. The results for each group are presented in a separate subsection.

5.1 Thermal properties of the material

All thermal properties c , ρ , and λ of the material in Eqs 2 and 5, depend on the current temperature at a particular point in the probe. During the numerical solution of the HCE, they have to be adjusted repeatedly, to reflect the correct thermal behavior. Therefore, the HTC calculation contains an additional loop (step 3 of the algorithm) to perform this adjustment by simple iterations. As a consequence, the whole computation is slowed down significantly.

In order to speed up the calculation, it is quite popular in practice to take constant values of thermal properties at some fixed temperature. One of the objectives of this test is to see how that affects the solution. The output curves are computed by taking all thermal properties for Inconel 600 as constant values, first at the room temperature of 30 °C, and then at 400 °C, which is much closer to the actual temperature of intensive cooling. This test, of course, is impossible to do in practice, but it is essential for the HTC calculation procedure.

On the other hand, for practical applications, it is far more interesting to see what happens when the material of the probe is changed from one steel to another, which

is quite expensive to do in real life. So, in the third test, the probe is considered to be made of AISI 304 stainless steel, instead of Inconel 600. Because AISI 304 is composed mostly of iron, the actual thermal properties are somewhat different at the same temperatures [1], but both steels exhibit quite similar behavior when quenched.

The results of these three tests for quenching in oil are shown in Figs. 7–10, and in Figs. 11–14, for quenching in water.

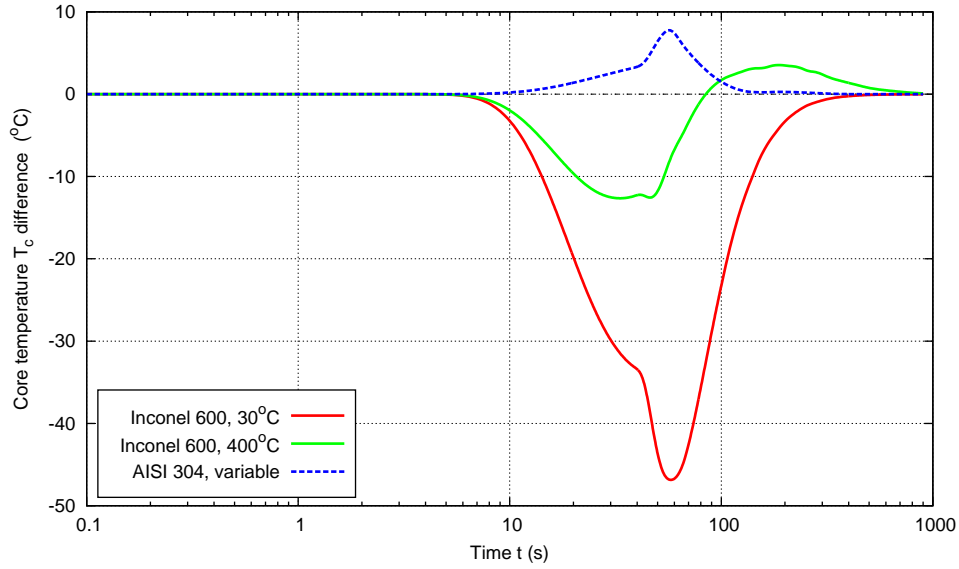


Fig. 7 Oil (thermal properties variation): core temperature T_c differences.

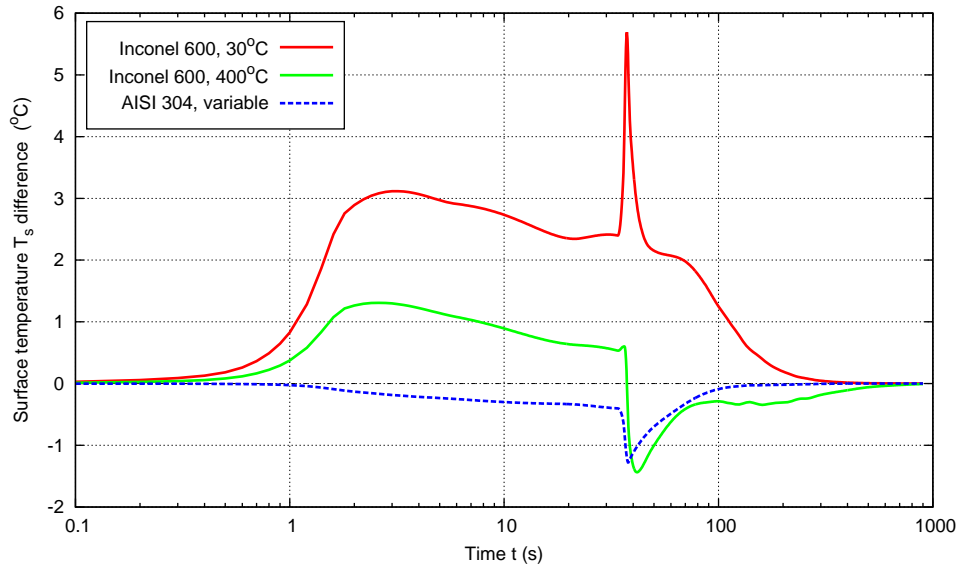


Fig. 8 Oil (thermal properties variation): surface temperature T_s differences.

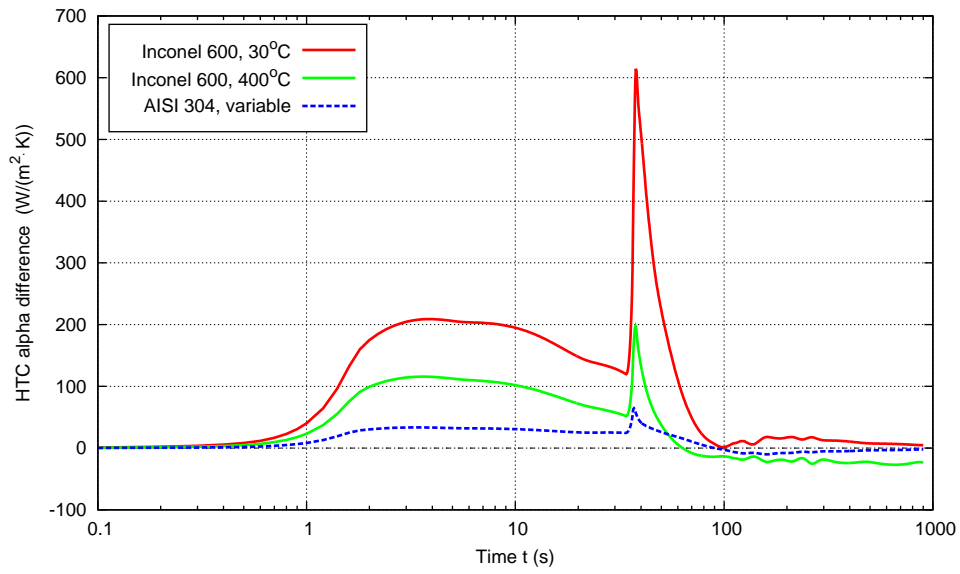


Fig. 9 Oil (thermal properties variation): HTC α differences.

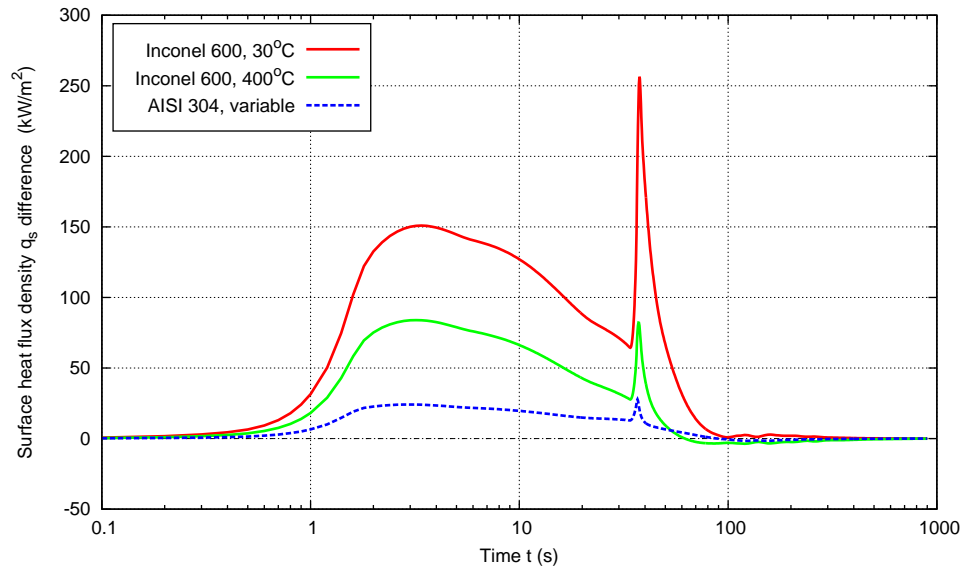


Fig. 10 Oil (thermal properties variation): surface heat flux density q_s differences.

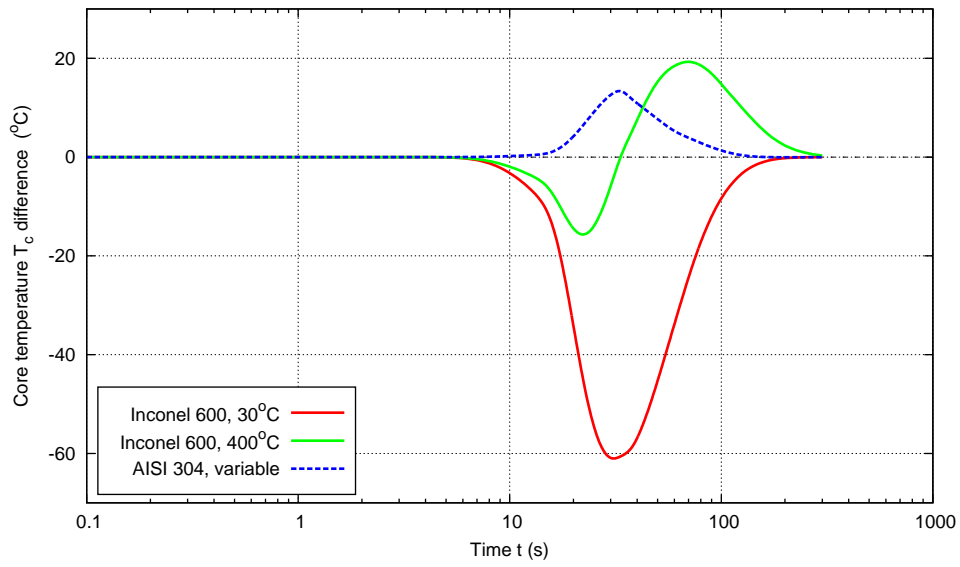


Fig. 11 Water (thermal properties variation): core temperature T_c differences.

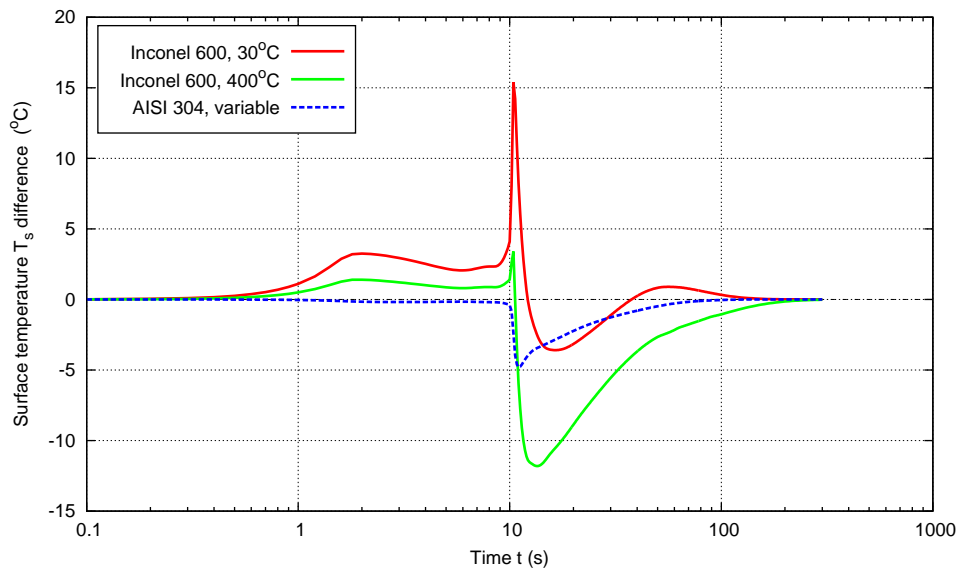


Fig. 12 Water (thermal properties variation): surface temperature T_s differences.

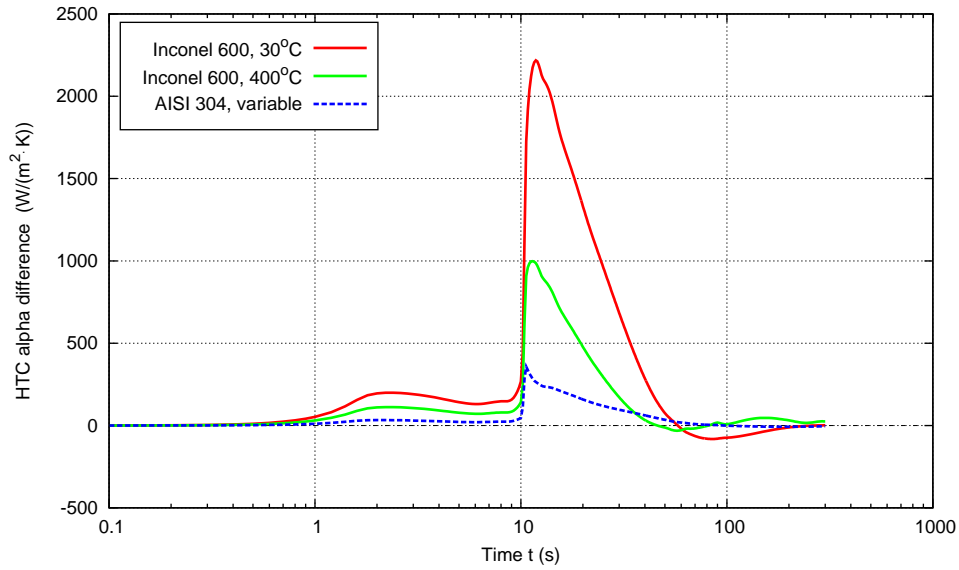


Fig. 13 Water (thermal properties variation): HTC α differences.

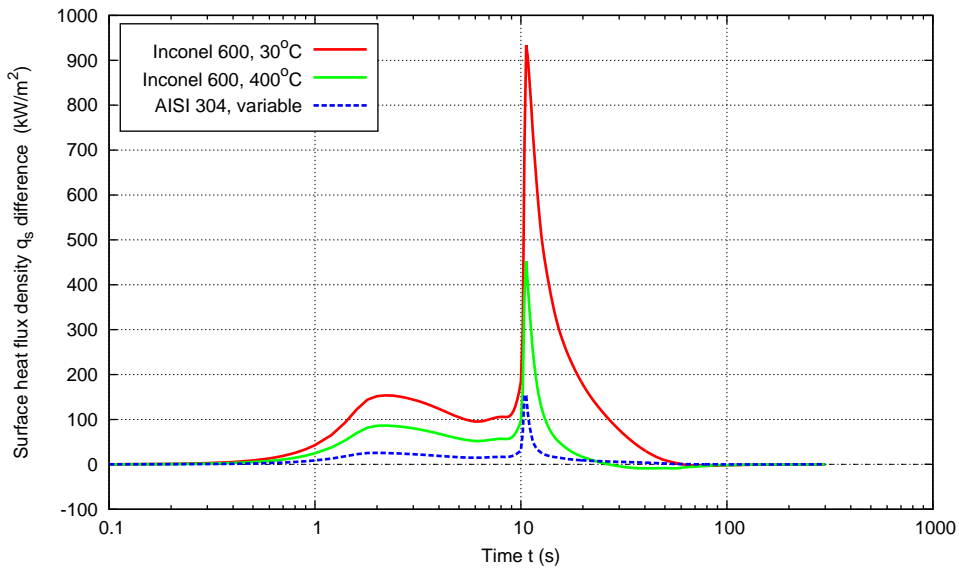


Fig. 14 Oil (thermal properties variation): surface heat flux density q_s differences.

In all output curves, the highest differences occur during the most intensive cooling period, and this behavior is typical for all subsequent tests, as well. Constant thermal properties, especially at the room temperature, result in very high differences. For example, the peak HTC values, both in oil and water, are underestimated by about 25%. The test definitely shows that all thermal properties must be considered as temperature-dependent in quenching simulations.

More interestingly, the change of the material by another steel that is known to have similar quenching characteristics, results in relatively small differences in all output curves, i.e., the simulation confirms that they are similar (which verifies the simulation itself). This comment is valid only for similar steels, and a completely different steel would result in much higher differences, but the point is that they can be predicted by simulation.

5.2 Near-surface thermocouple depth

The reference curves are computed from the near-surface temperature T_n measured at the depth $d_n = 1$ mm below the surface. When the probe is manufactured, it is quite hard to achieve the exact drilling and positioning of the near-surface thermocouple, and some small differences in the depth can be expected in practice. Moreover, the diameter of the thermocouple is about 1 mm, and it is very hard to tell what is the actual depth that corresponds to the measured temperature T_n .

The goal of this test is to study the effects of the depth variation, and six different depths d_n are used, with the step of 0.1 mm, three of them above, and three below the standard position. The same near-surface temperature curve $T_n(t)$ is used, as in the reference results, even though it is very unlikely that the same temperature curve would be measured at different positions in the same quenching conditions. This is the only sensible thing to do, without actually doing the experiments with such probes. Besides, the aim is to analyze the sensitivity with respect to the depth, so only d_n should be varied.

The results of all six tests for quenching in oil are shown in Figs. 15–18, and the results in water are shown in Figs. 19–22.

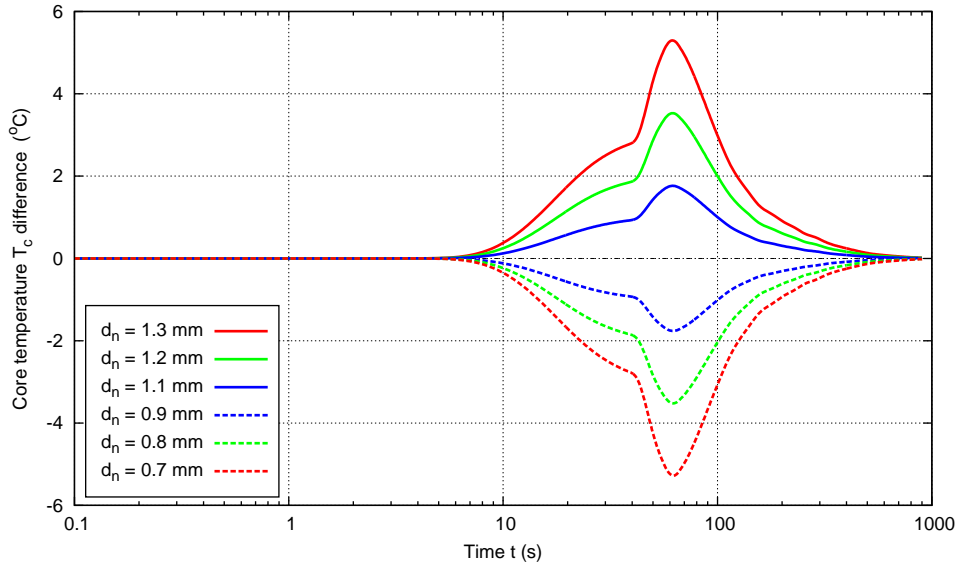


Fig. 15 Oil (thermocouple depth variation): core temperature T_c differences.

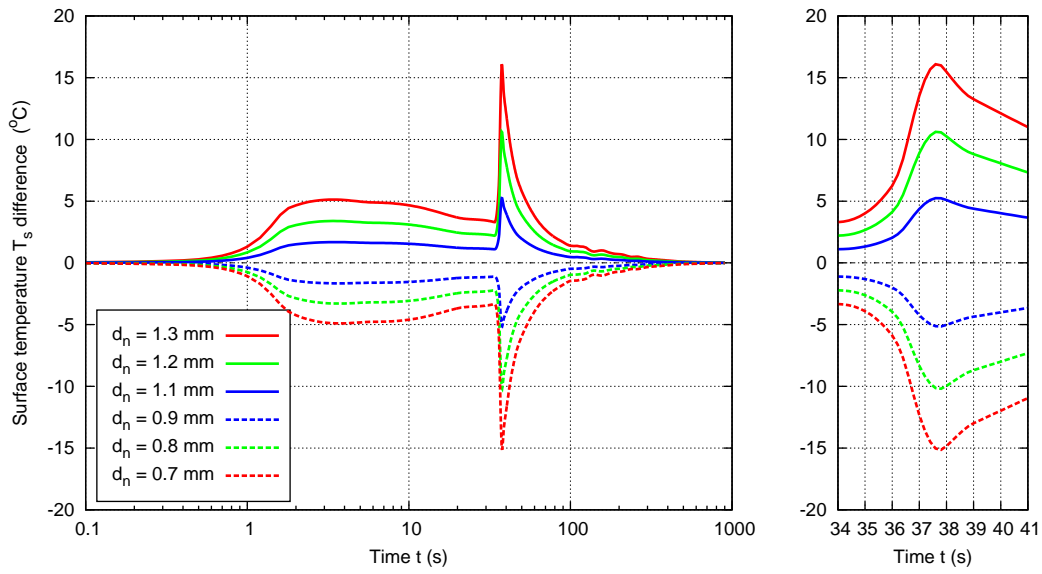


Fig. 16 Oil (thermocouple depth variation): surface temperature T_s differences.

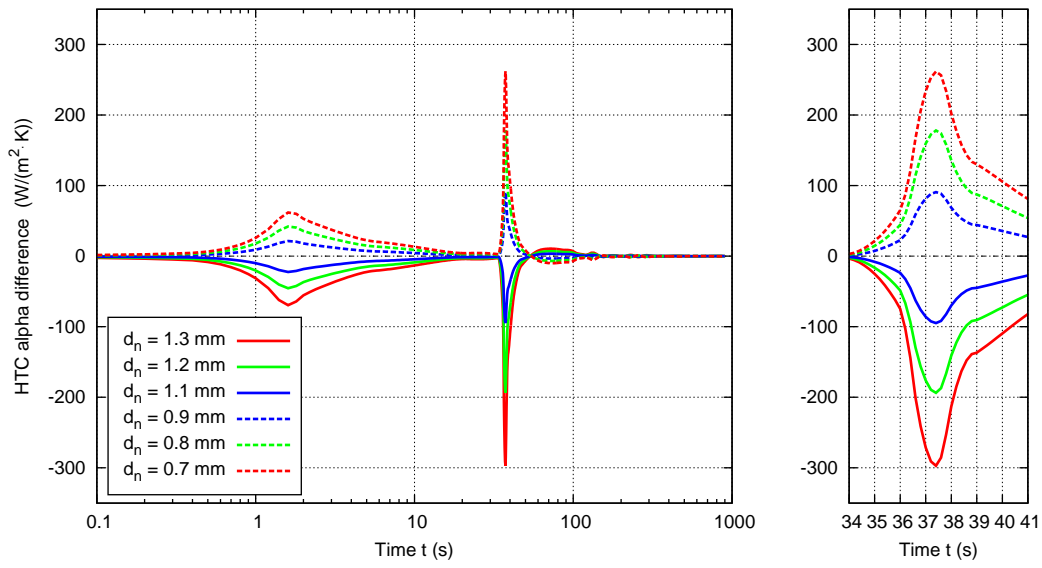


Fig. 17 Oil (thermocouple depth variation): HTC α differences.

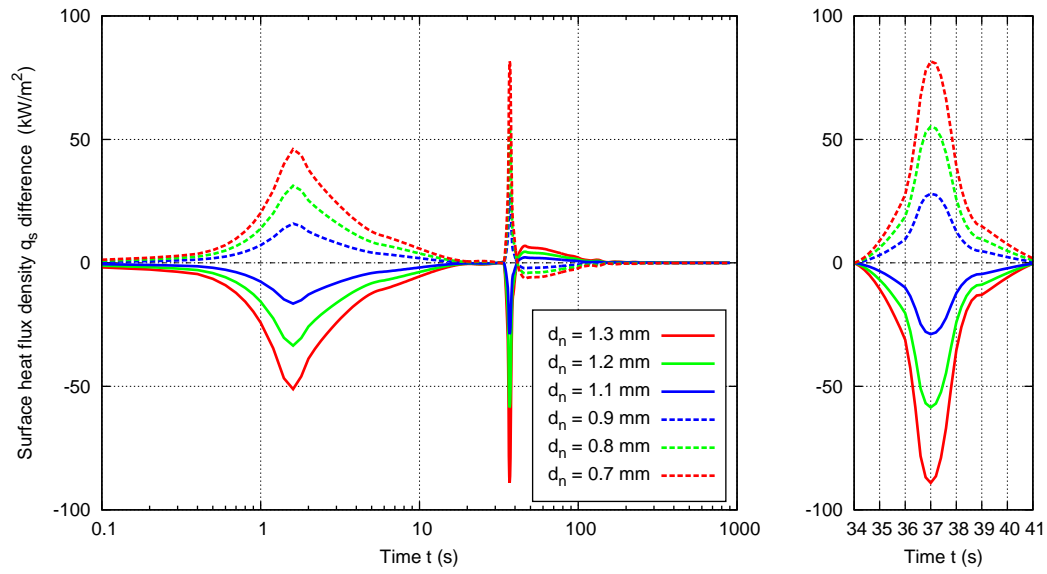


Fig. 18 Oil (thermocouple depth variation): surface heat flux density q_s differences.

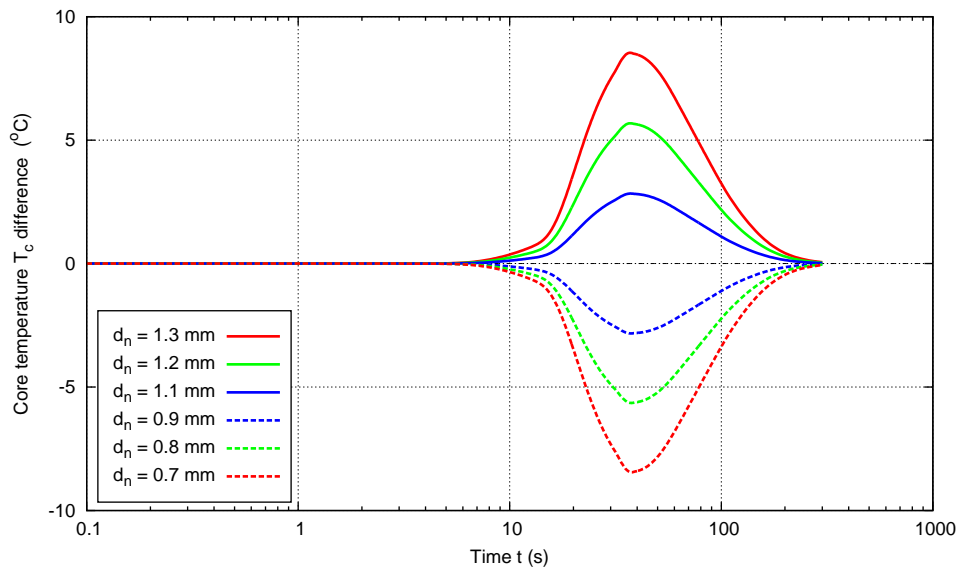


Fig. 19 Water (thermocouple depth variation): core temperature T_c differences.

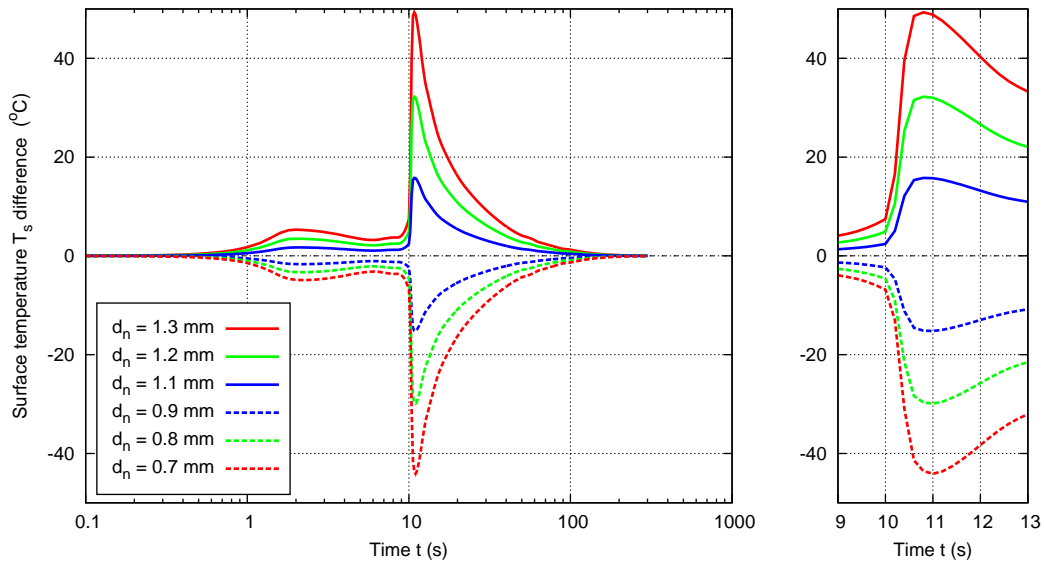


Fig. 20 Water (thermocouple depth variation): surface temperature T_s differences.

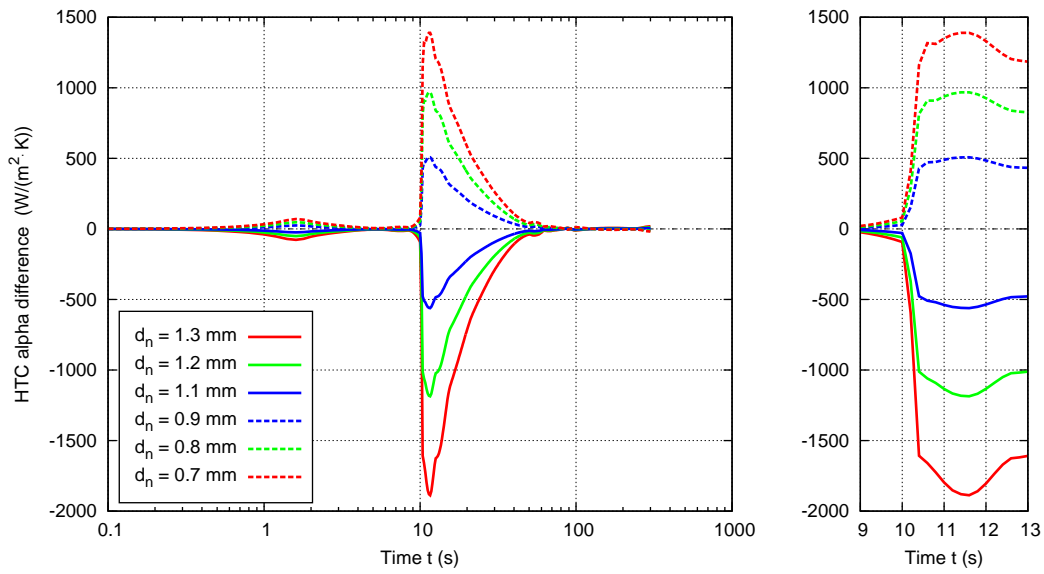


Fig. 21 Water (thermocouple depth variation): HTC α differences.

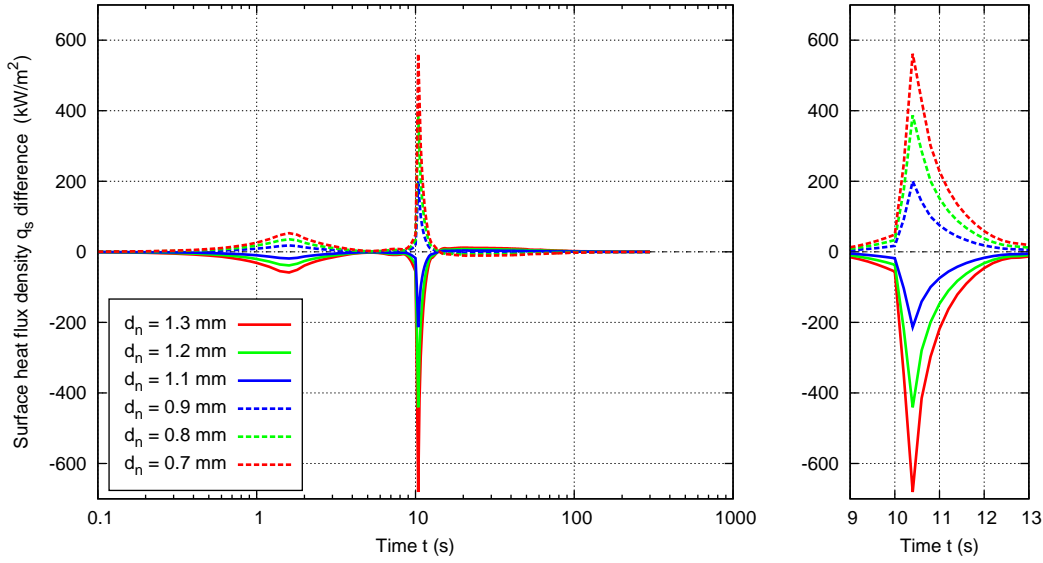


Fig. 22 Water (thermocouple depth variation): surface heat flux density q_s differences.

The magnitudes of differences are higher in water: about 10°C for the core temperature T_c , more than 40°C for the surface temperature T_s , and the HTC differences range from $-2,000$ to $1,500 \text{ W}/(\text{m}^2 \cdot \text{K})$. The shape of the difference curves is similar, but they last longer, because of higher magnitudes.

Because the depth is quite small, and the changes of depth are relatively large, the resulting differences in the surface conditions, i.e., in T_s and α , are quite high. On the other hand, the depth changes are small with respect to the whole radius of the probe, and they happen far away from the core, so the core temperature T_c is only marginally affected.

5.3 Probe diameter

This group of tests may seem odd, since the diameter of the probe is fixed, and all reference curves are calculated with the diameter $D = 50 \text{ mm}$. However, there are at least two reasons why it is worth doing. Exactly because the diameter is fixed, someone may be tempted to use the same output curves for an actual piece of a different size, without being aware of the errors that might cause (it has been tried in practice). From a more positive point of view, this sensitivity test will give at least some indications about the possibility of using the results for other pieces, without actually doing the tests with different probes.

The tests are very similar to the previous group, except that a much larger step is used, to make the results more interesting for practical purposes. Six different diameters are tested, with the step of 5 mm . Three of them are smaller, and three are larger than the standard diameter. Like before, only the diameter D is varied, with the same input curve $T_n(t)$. Here, of course, it is virtually impossible that the same temperature would be measured at the same depth (1 mm) in similar quenching conditions, so the results should be interpreted with this in mind.

The results of all six tests for quenching in oil are shown in Figs. 23–26, and the results in water are shown in Figs. 27–30. The magnitudes of differences in oil are lower: about 130°C for the core temperature T_c , about 5°C for the surface temperature T_s , and the HTC differences range from -400 to $500\text{ W}/(\text{m}^2 \cdot \text{K})$. The shape of all difference curves is very similar, except that the HTC differences diminish towards the end of the process, i.e., they behave more regularly than in water.

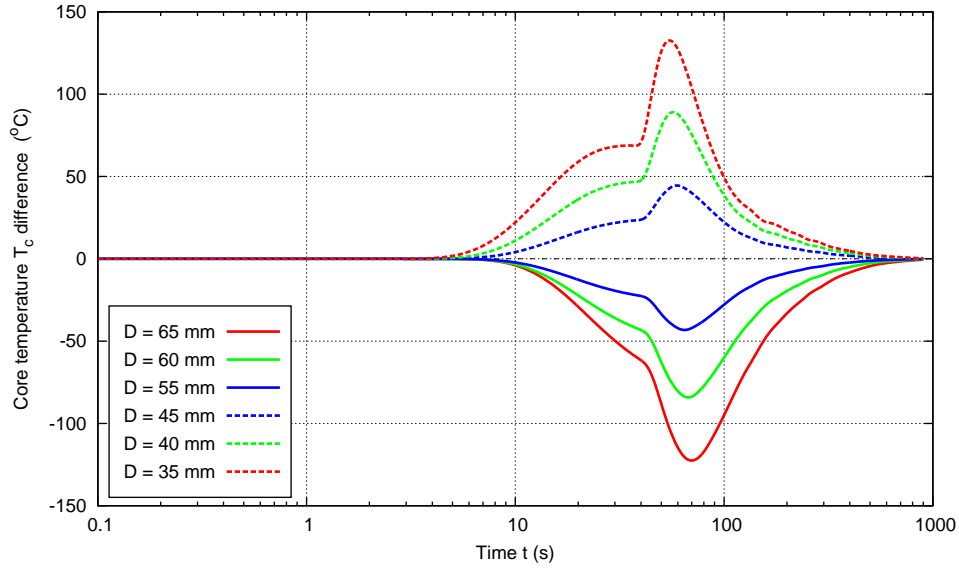


Fig. 23 Oil (diameter variation): core temperature T_c differences.

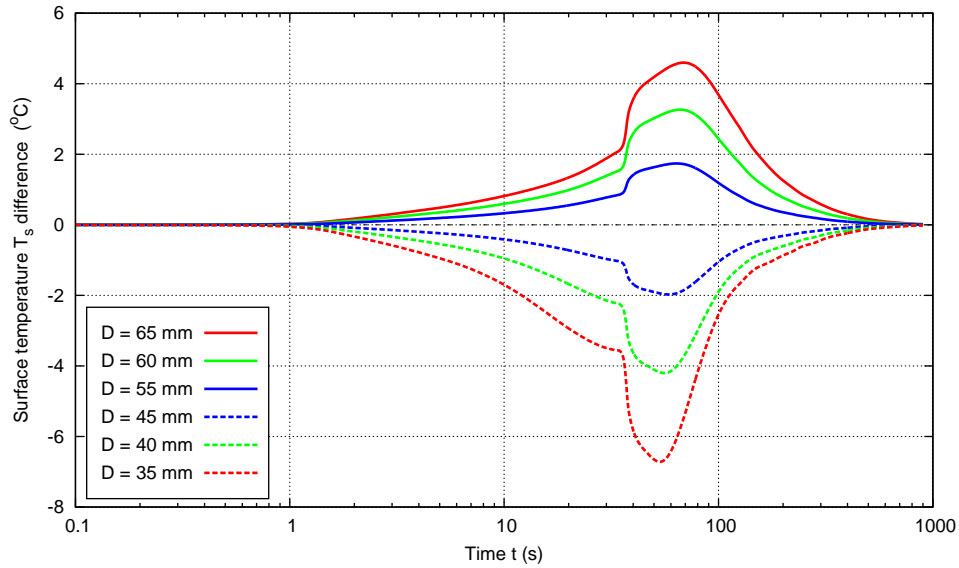
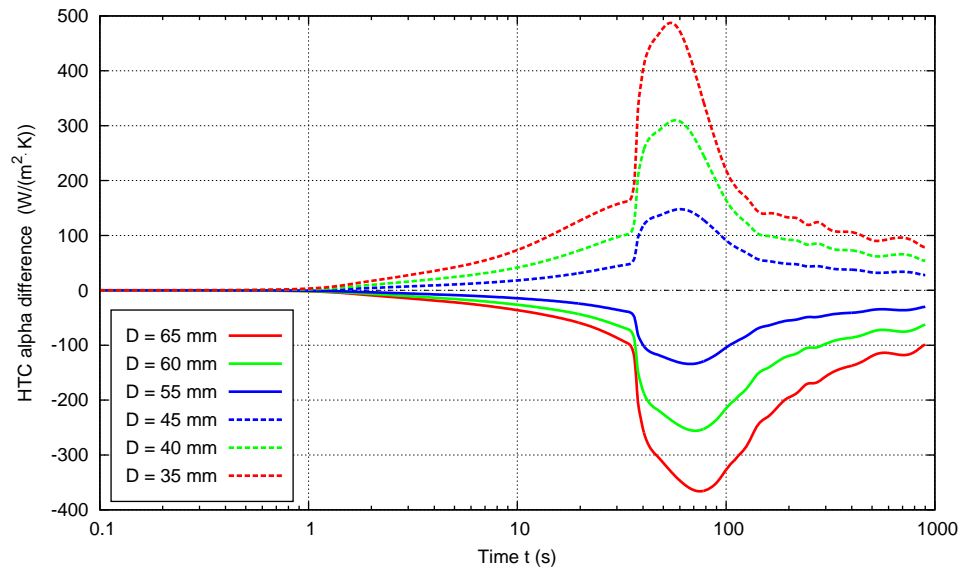
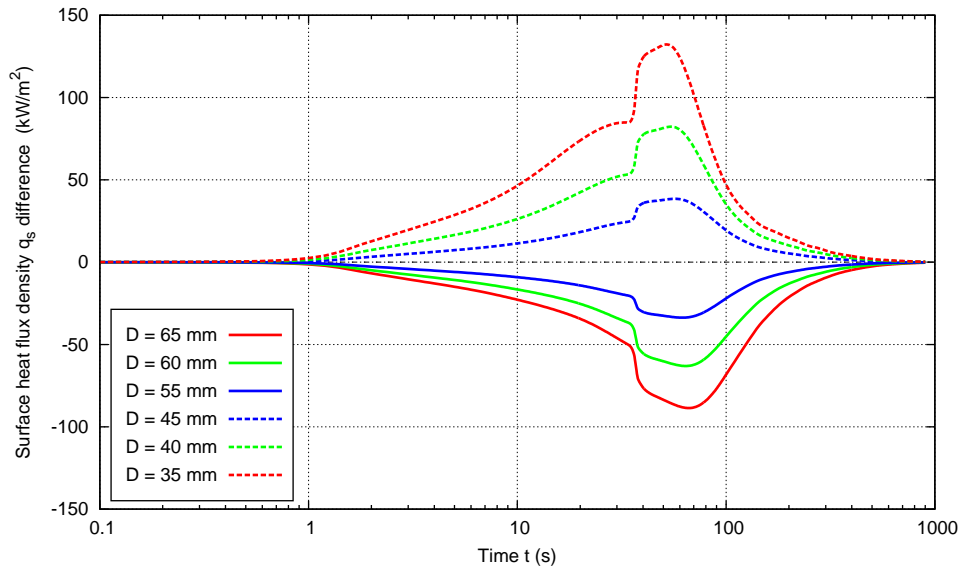


Fig. 24 Oil (diameter variation): surface temperature T_s differences.

Fig. 25 Oil (diameter variation): HTC α differences.Fig. 26 Oil (diameter variation): surface heat flux density q_s differences.

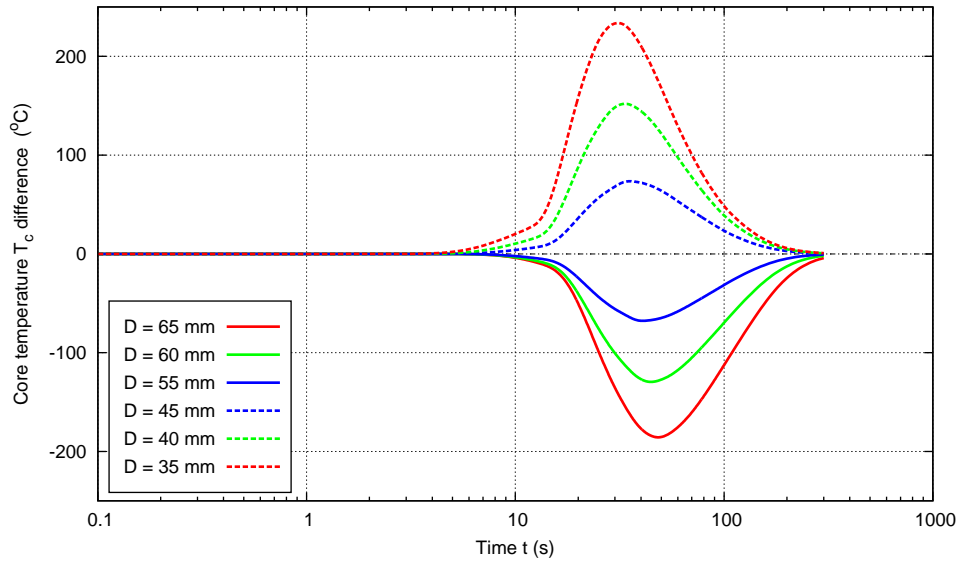


Fig. 27 Water (diameter variation): core temperature T_c differences.

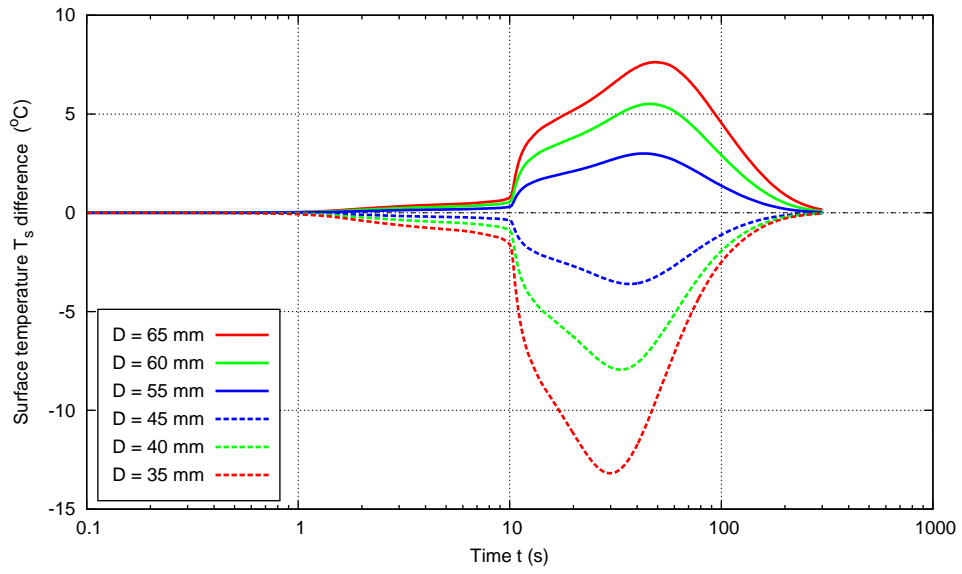


Fig. 28 Water (diameter variation): surface temperature T_s differences.

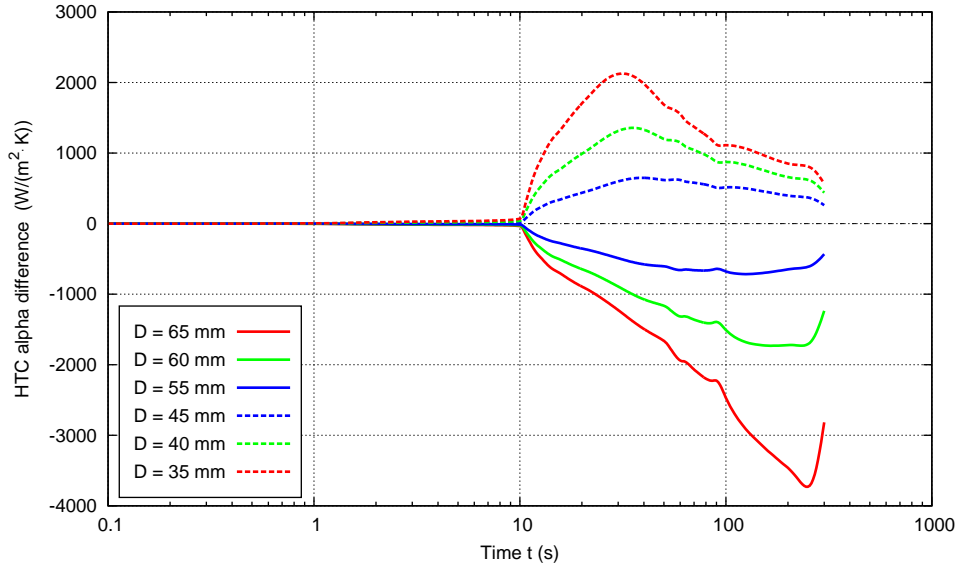


Fig. 29 Water (diameter variation): HTC α differences.

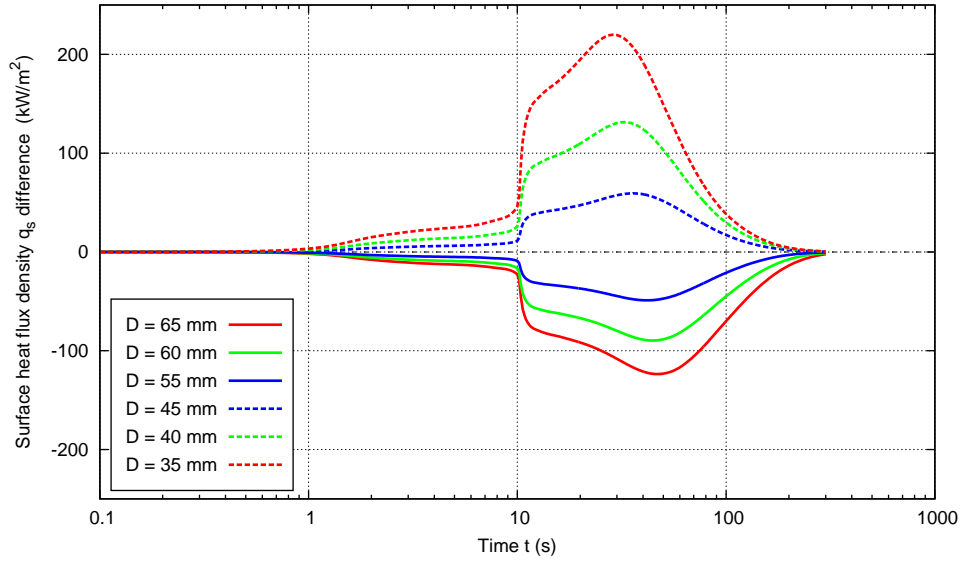


Fig. 30 Water (diameter variation): surface heat flux density q_s differences.

The results here are quite the opposite from those in the previous group. Because the depth d_n is fixed, any change of the diameter effectively changes the distance of the near-surface thermocouple from the core. Therefore, it is reflected mostly in the core temperature. The surface conditions are less affected, especially the surface temperature. The HTC differences are large because of relatively large changes of the diameter.

Moreover, the HTC results in Fig. 29 demonstrate a phenomenon that can occur with the HTC curves calculated in water—the values at the very end of the quenching process can blow up, with no apparent limit. Surface heat flux densities in Fig. 30 do not exhibit this behavior, and their values (as well as differences with respect to the original unperturbed values) nicely tend to zero for high times. The explanation for

high, possibly unbounded, HTC values for high times comes from Eq 4, where the HTC is calculated as

$$\alpha = \frac{q_s}{T_s - T_x}. \quad (6)$$

The denominator, i.e., the difference between the surface and the quenchant temperatures, also tends to zero for high times, and there is no apparent physical reason that the HTC should be bounded at the time limit.

Finally, actual experiments with probes having different diameters, from 20 mm to 80 mm, but of the same design, and in the same quenching conditions, reported in [9, 20], show that the HTC curves are more similar than the sensitivity results suggest. For very small diameters, this is not true any more, and the HTC sharply increases.

5.4 Space step

The last two groups of tests are intended to verify the reliability of the HTC calculation with respect to the main numerical parameters of the method—the space step and the time step, that are used in the discretization of the heat conduction problem.

In the FVM, the whole radius of the probe is divided into a certain number of finite volumes that determine the space grid, and temperatures are calculated only at the points of this grid. The grid points are uniformly spaced, with the space step h (mm), except possibly at the center. Because the method is based on the solution extension over the interval $[R - d_n, R]$, the near-surface thermocouple position $R - d_n$ is always taken as the grid point, so that the corresponding temperature is calculated directly in step 4, without any additional interpolation. Therefore, the space step h is determined as

$$h = \frac{d_n}{N_{\text{ext}}}, \quad (7)$$

where N_{ext} is the prescribed number of the so-called extension intervals—that many intervals of length h are located between the near-surface position and the surface. As a result, the central volume may be twice as wide, to get an integral number of intervals (volumes) over the whole radius.

Usually, the results are computed with $N_{\text{ext}} = 8$ extension intervals, or with the space step $h = 0.125$ mm, giving a total of 200 volumes over the radius of the probe. In this group of tests, the following four values of N_{ext} are taken in Eq 7:

$$N_{\text{ext}} = 1, 2, 4, 10. \quad (8)$$

The space step h varies from 0.1 mm to 1.0 mm, and the total number of volumes varies from 25 to 250.

The results of all four tests for quenching in oil are shown in Figs. 31–34, and the results in water are shown in Figs. 35–38. Even with the largest space step, the resulting differences in both temperatures are very small: less than 0.06°C for oil, and less than 0.8°C for water.

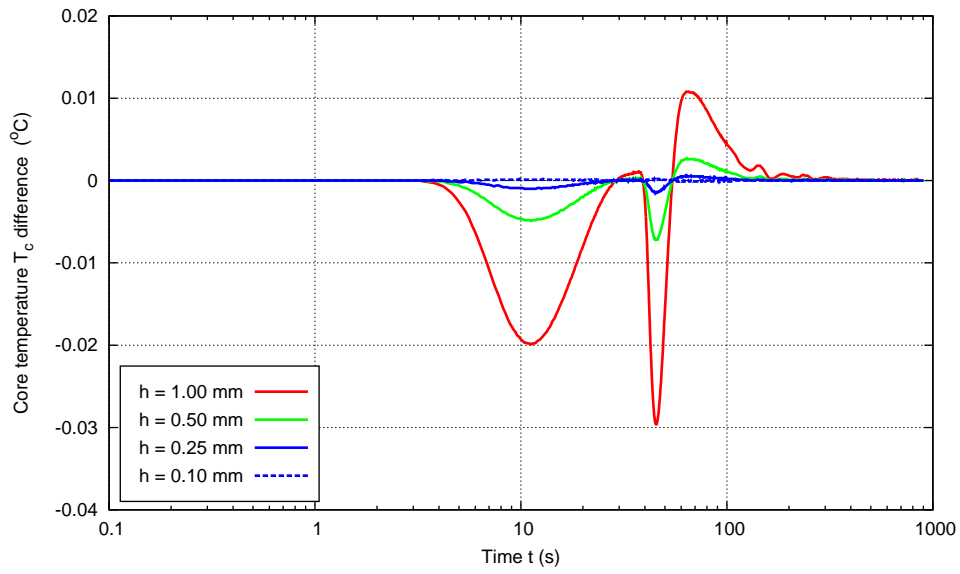


Fig. 31 Oil (space step variation): core temperature T_c differences.

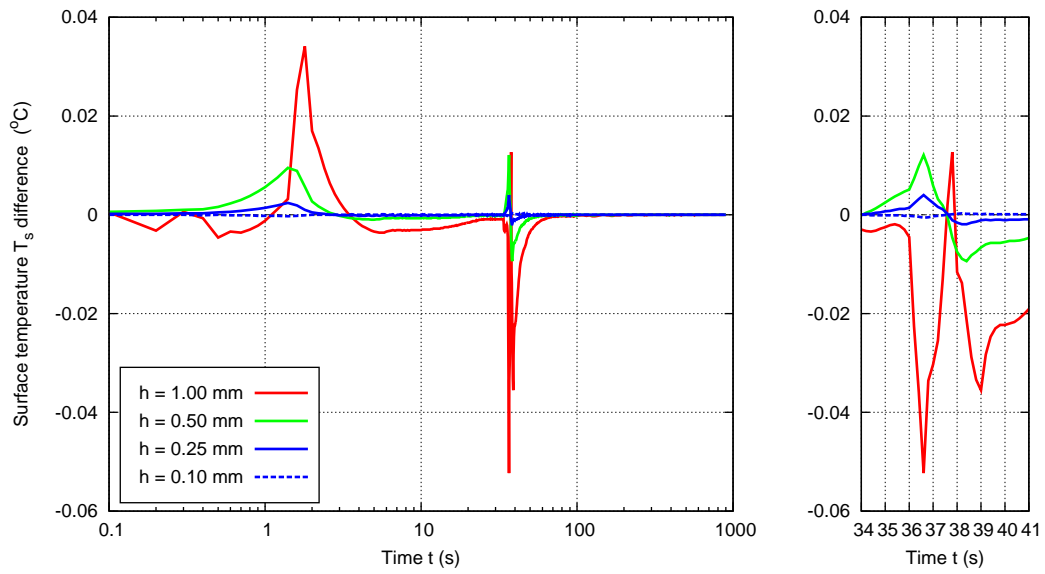
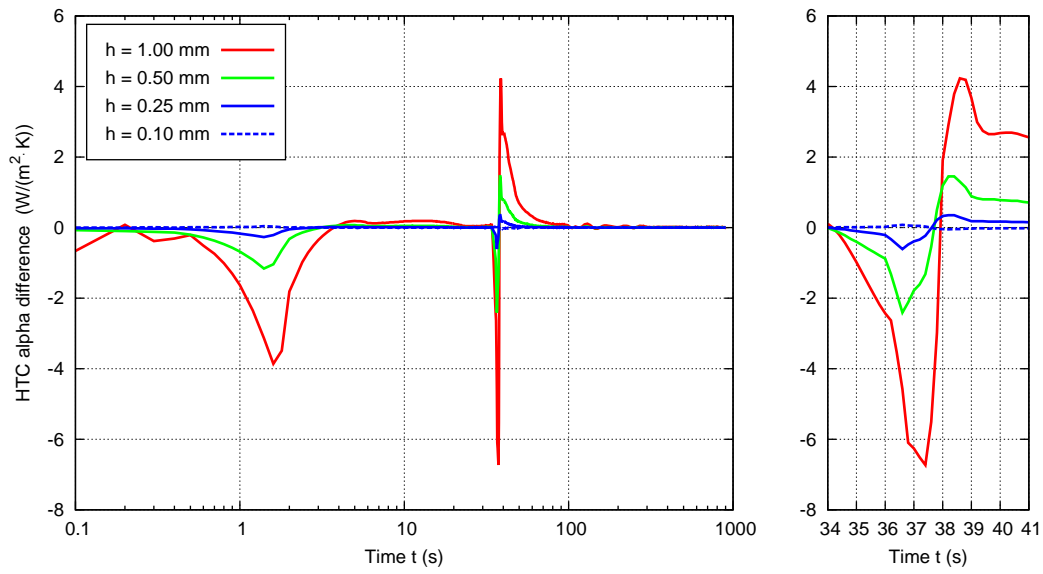
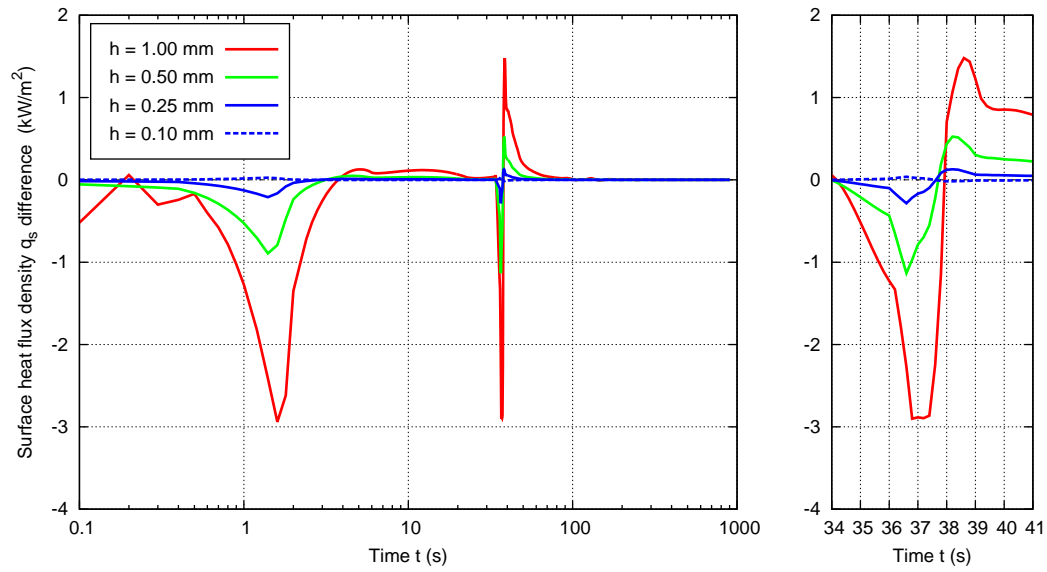


Fig. 32 Oil (space step variation): surface temperature T_s differences.

Fig. 33 Oil (space step variation): HTC α differences.Fig. 34 Oil (space step variation): surface heat flux density q_s differences.

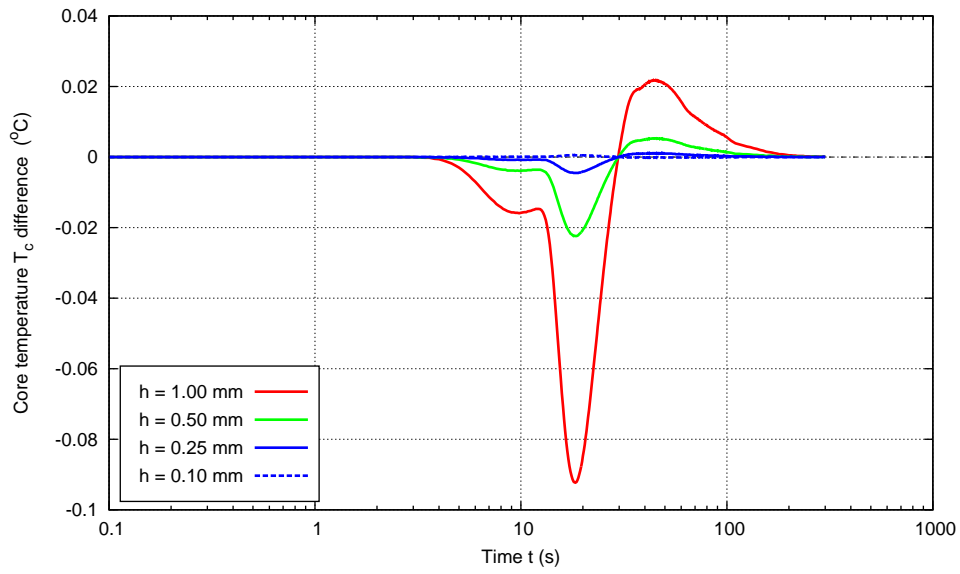


Fig. 35 Water (space step variation): core temperature T_c differences.

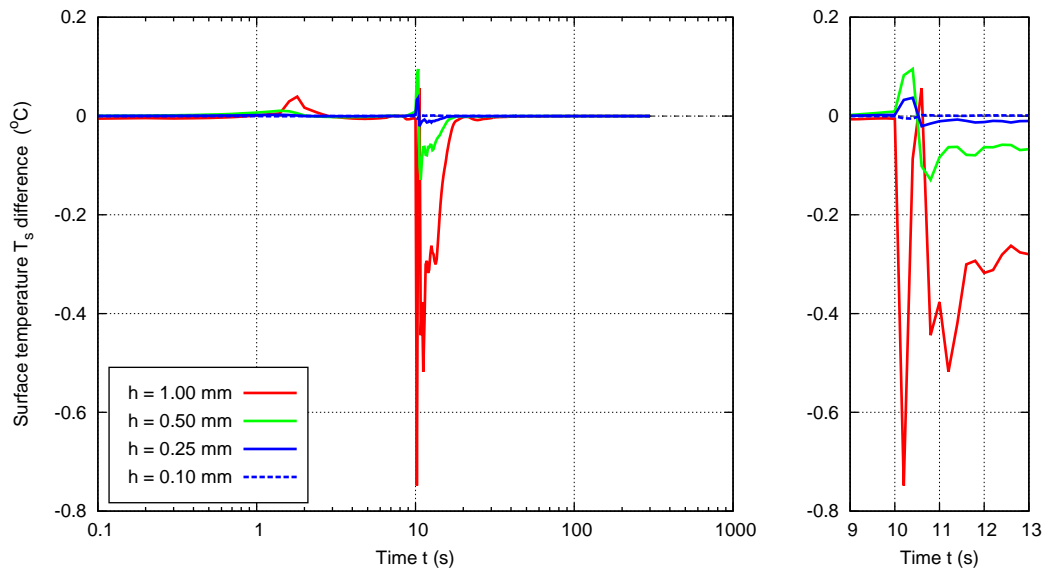
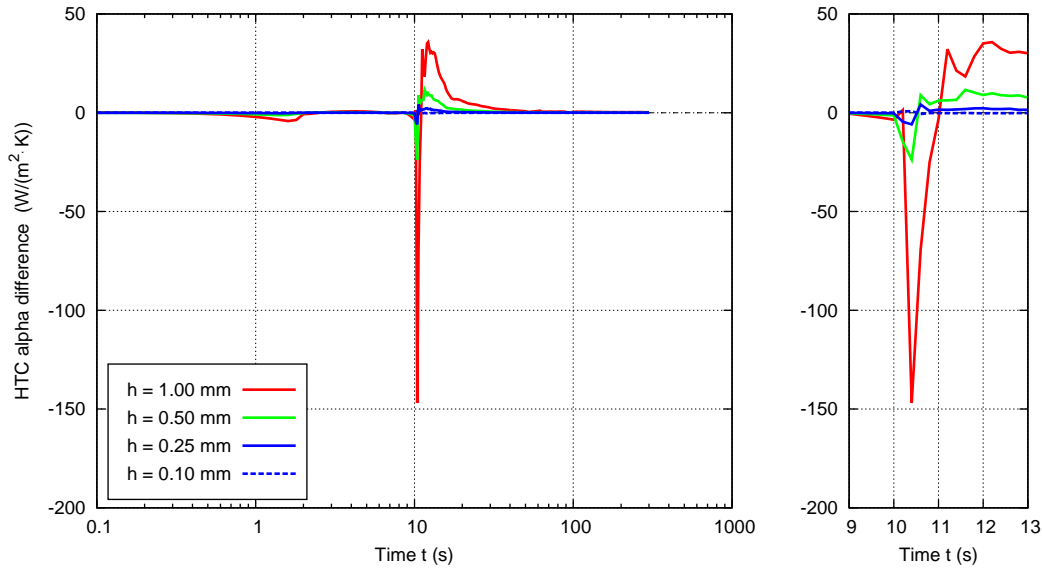
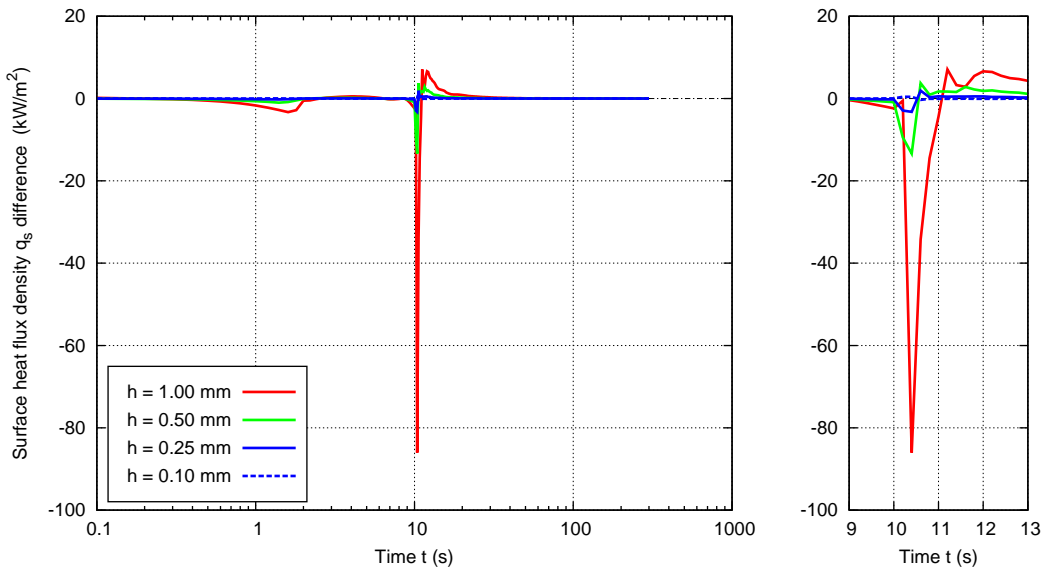


Fig. 36 Water (space step variation): surface temperature T_s differences.

Fig. 37 Water (space step variation): HTC α differences.Fig. 38 Water (space step variation): surface heat flux density q_s differences.

High differences in the HTC are strictly confined to the intensive cooling period, and large peaks are obtained only when a single extension interval is used. In all other cases, the differences may be considered as negligible, for all practical purposes.

The method becomes slightly less stable with a very large number of extension intervals ($N_{\text{ext}} \geq 12$), and the usual value of 8 extension intervals turns out to be a good choice.

5.5 Time step

The overall space accuracy of the method is reasonably high, proportional to h^2 . In contrast to that, because it is based on the implicit advance in time, its accuracy

with respect to time is quite low, directly proportional to the time step. So, despite the fact that large time steps can be used without a sacrifice in stability, they still have to be chosen with some care to preserve the accuracy of the computed solution.

In order to speed up the calculation, different time steps τ_i are used in different periods of the quenching process. The computation begins with the finest time step, denoted by τ (s), that is used throughout the most intensive part of the process. For the standard probe, this time step is used for the first 100 seconds. Later on, when the temperature drops, much coarser time steps are used.

The standard value for the finest time step is $\tau = 0.02$ s, in accordance with the frequency of measurements gathered by the probe. All the results presented thus far, have been computed with this time step. In this group of tests, the following values of the finest time step are used:

$$\tau = 0.01, 0.025, 0.05, 0.1 \text{ s.} \quad (9)$$

The first one is finer than the standard step, while the last one is five times coarser.

The results of these tests for quenching in oil are shown in Figs. 39–42, and the results in water are shown in Figs. 43–46. Similarly to the previous group, even with the largest time step, the resulting differences in both temperatures are quite small: about 0.6°C for oil, and less than 7.0°C for water.

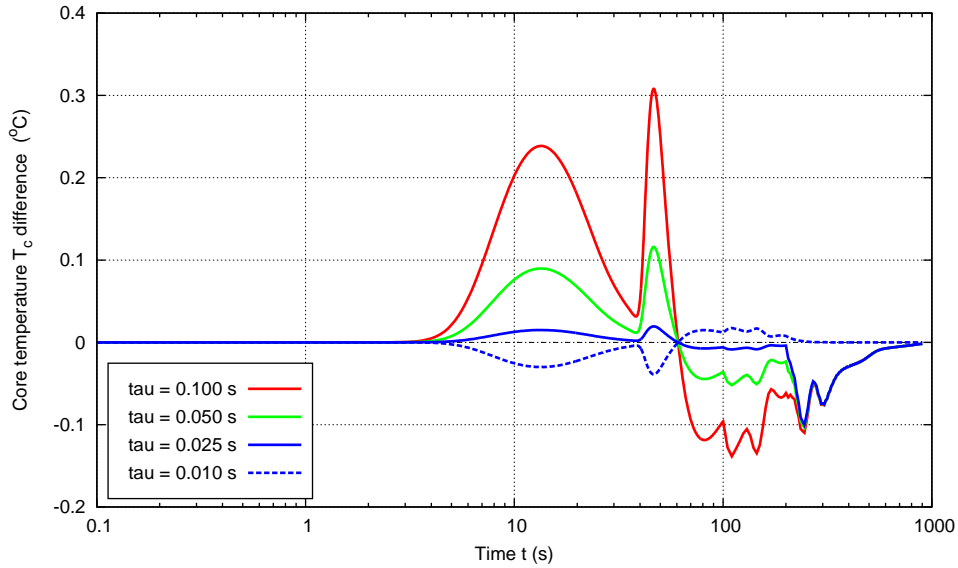
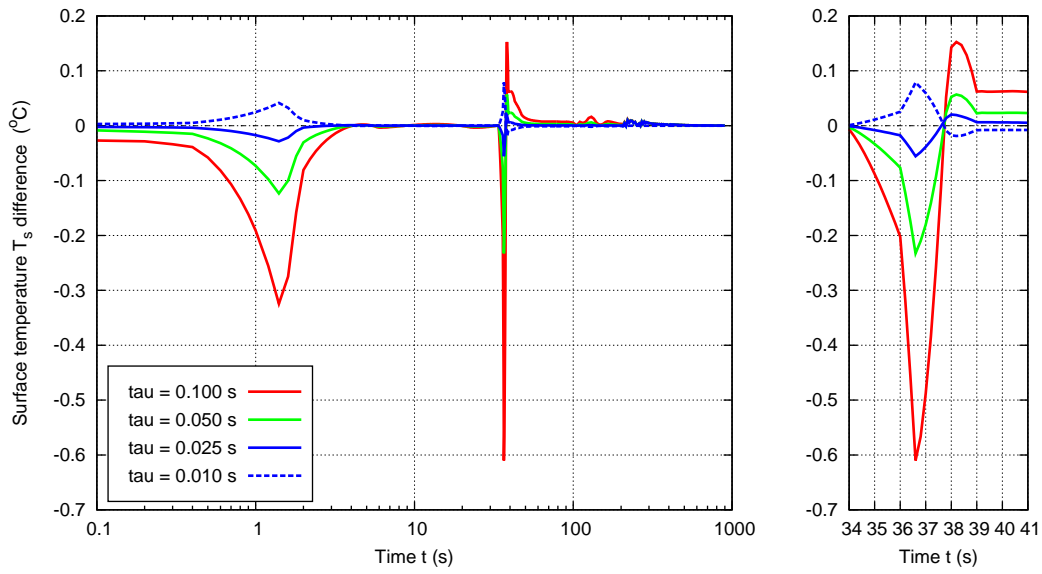
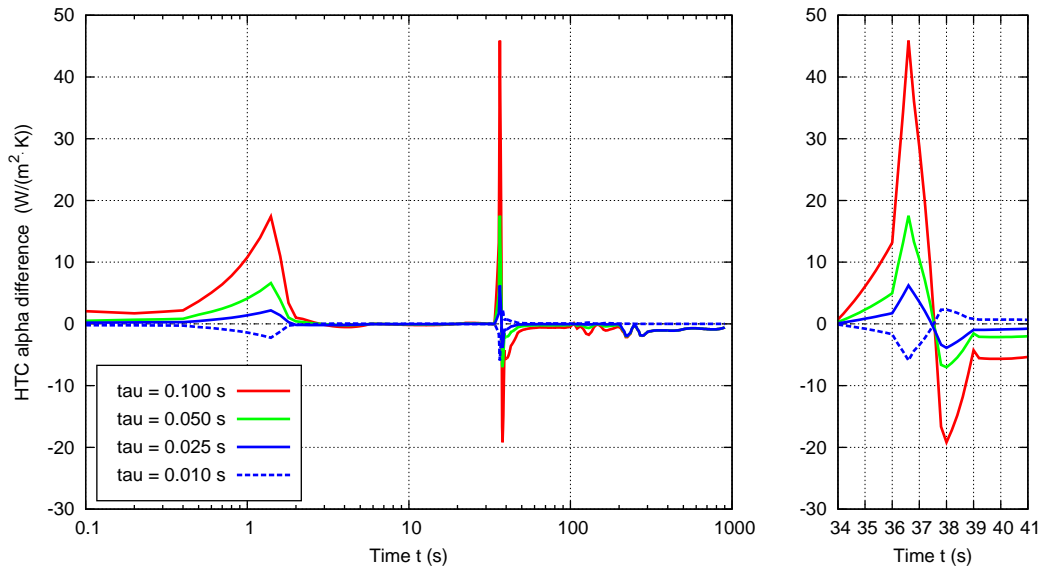


Fig. 39 Oil (time step variation): core temperature T_c differences.

Fig. 40 Oil (time step variation): surface temperature T_s differences.Fig. 41 Oil (time step variation): HTC α differences.

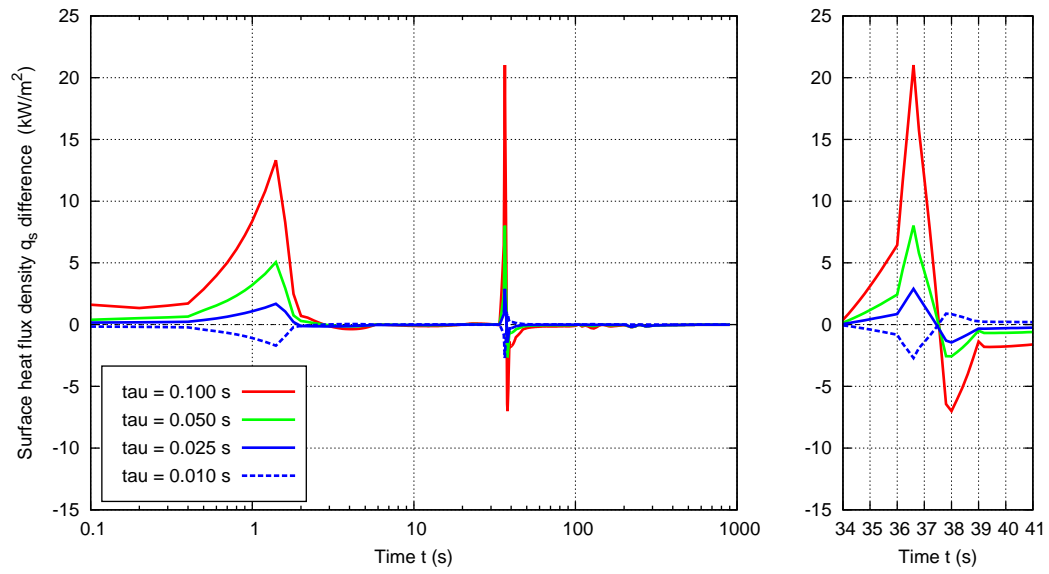


Fig. 42 Oil (time step variation): surface heat flux density q_s differences.

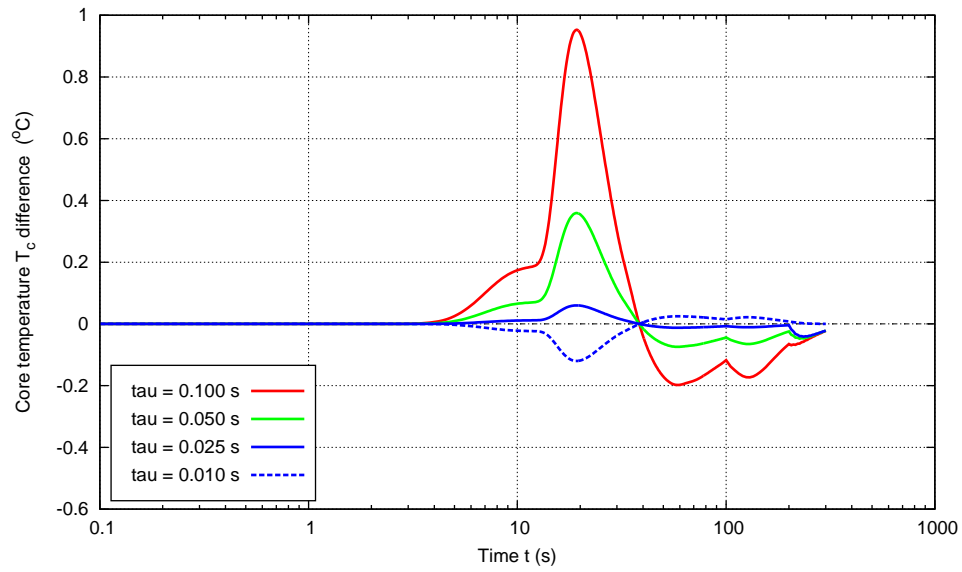


Fig. 43 Water (time step variation): core temperature T_c differences.

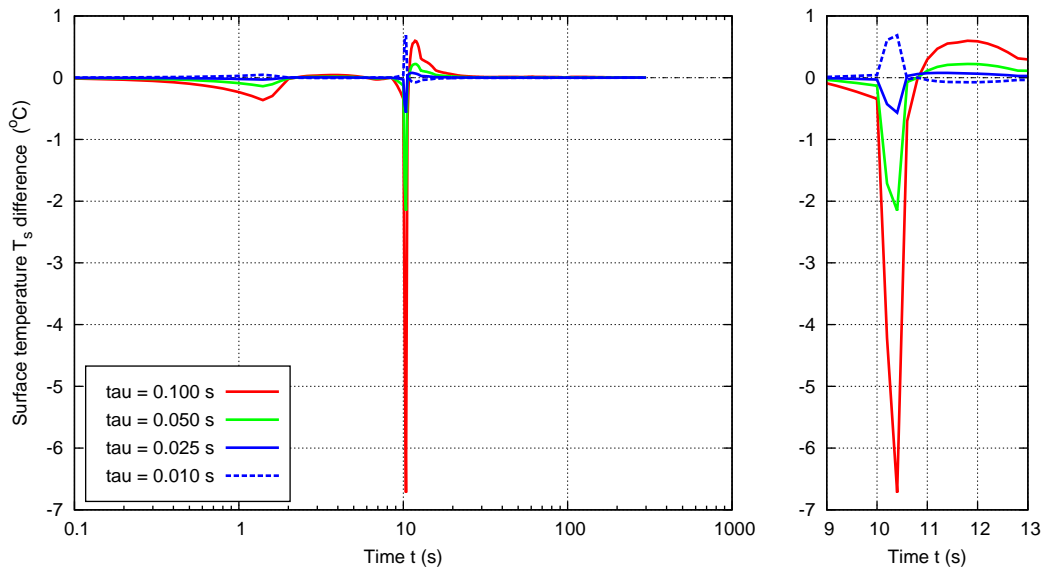


Fig. 44 Water (time step variation): surface temperature T_s differences.

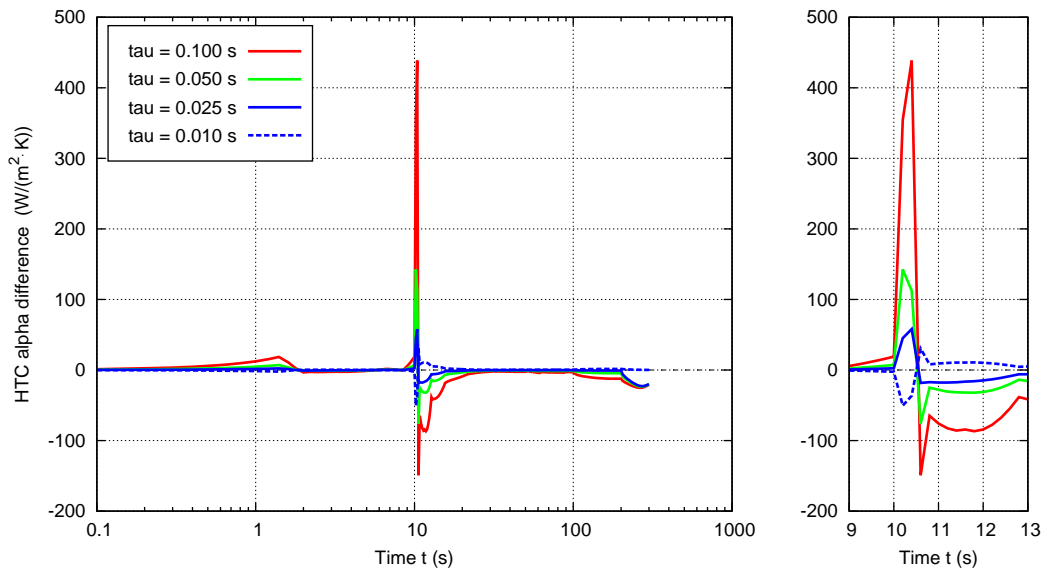


Fig. 45 Water (time step variation): HTC α differences.

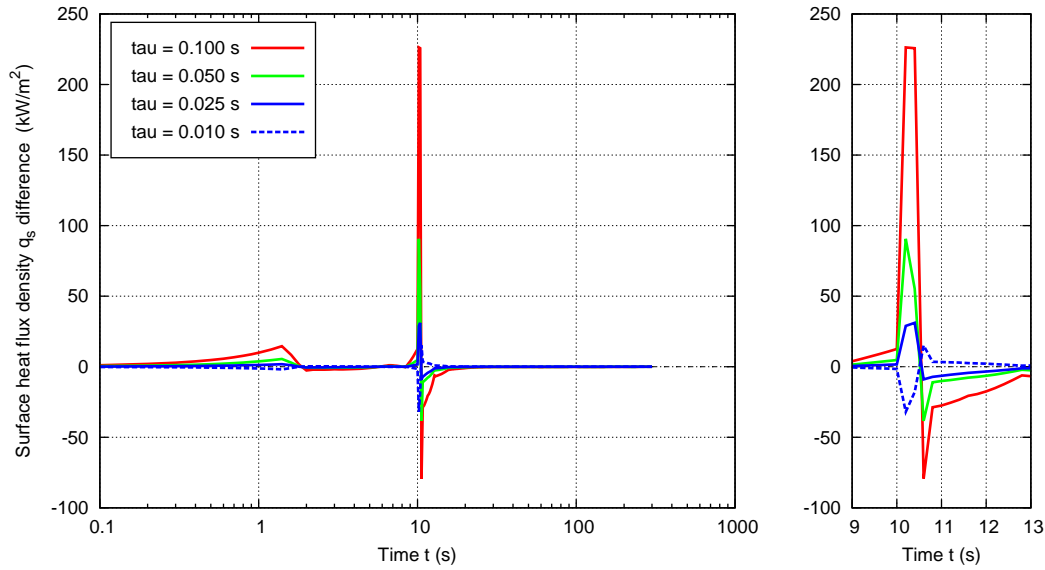


Fig. 46 Water (time step variation): surface heat flux density q_s differences.

Again, high differences in the HTC are strictly confined to the intensive cooling period. However, for the largest time step, the peak differences are equivalent to the relative error of about 5% in the corresponding peak HTC values. Therefore, time steps much larger than the standard step should not be used for the HTC calculation.

During the course of these tests, several other methods for the solution of the IHCP have been tested, as well. For example, the finite difference method [21] gives very similar results, with the same discretization parameters, provided that an accurate algorithm for numerical differentiation is used to calculate the surface heat flux density.

6 Conclusion

Several numerical experiments have been performed to test the sensitivity of the HTC calculation with respect to the main input parameters of the problem, including the numerical discretization parameters involved in numerical solution of the problem.

The results confirm that the numerical procedure itself is reliable and numerically stable, so it can be used for the solution of the IHCP to obtain reasonably accurate HTC curves, from properly prepared data. The measured temperature curves have to be adequately smoothed, and thermal properties of the material must be temperature-dependent to obtain good results.

All sensitivity tests have been conducted with realistic cooling curves from two quenchants, and the results with respect to the position of the near-surface thermocouple, and the diameter of the probe, may provide some interesting information about the behavior of the HTC in various liquid quenchants.

References (in the order of citation)

- [1] Totten, G. E., Dossett, J. L. and Kobasko, N. I., “Quenching of Steel”, *ASM Handbook*, Volume 4A, *Steel Heat Treating Fundamentals and Processes*, J. Dossett and G. E. Totten, Eds., ASM International, Materials Park, OH, 2013, pp. 91–157.
- [2] Liščić, B. and Singer, S., “Large Probes for Characterization of Industrial Quenching Processes”, *ASM Handbook*, Volume 4A, *Steel Heat Treating Fundamentals and Processes*, J. Dossett and G. E. Totten, Eds., ASM International, Materials Park, OH, 2013, pp. 176–191.
- [3] Hernández-Morales, B., “Characterization of Heat Transfer during Quenching”, *ASM Handbook*, Volume 4A, *Steel Heat Treating Fundamentals and Processes*, J. Dossett and G. E. Totten, Eds., ASM International, Materials Park, OH, 2013, pp. 158–175.
- [4] Smoljan, B., “Numerical Simulation of As-Quenched Hardness in a Steel Specimen of Complex Form”, *Commun. Numer. Meth. Eng.*, Vol. 14, 1998, pp. 277–285.
- [5] Smoljan, B., “Numerical Simulation of Steel Quenching”, *J. Mater. Eng. Perform.*, Vol. 11, No. 1, 2002, pp. 75–80.
- [6] Liščić, B., Singer, S. and Smoljan, B., “Prediction of Quench-Hardness within the Whole Volume of Axially Symmetric Workpieces of Any Shape”, *J. ASTM Int.*, Vol. 7, No. 2, 2010.
- [7] Tikhonov, A. N. and Arsenin, V. Y., *Solutions of Ill-Posed Problems*, V. H. Winston and Sons, Washington (distributed by Wiley, New York), 1977.
- [8] Beck, J. V., Blackwell, B. and St. Clair, Jr., C. R., *Inverse Heat Conduction, Ill-posed Problems*, Wiley-Interscience, New York, 1985.
- [9] Liščić, B. and Singer, S., “Calculation of the Heat Transfer Coefficient Based on Experiments by the Liscic Probes”, *Comprehensive Materials Processing*, S. Hashmi, Series Ed., Volume 12, *Thermal Engineering of Steel Alloy Systems*, G. Krauss, Ed., Elsevier Science, New York, 2014 (ISBN-978-0-08-096532-1, in press).
- [10] Felde, I., Réti, T., Sánchez Sarmiento, G., Palandella, M. G., Totten, G. E. and Chen, X. L., “Effect of Smoothing Methods on the Results of Different Inverse Modeling Techniques”, *Heat Treating: Including Quenching and Control of Distortion: An International Symposium in Honor of Professors Božidar Liščić and Hans M. Tensi*, Proceedings of the 21st Conference, 5–8 November 2001, Indianapolis, Indiana, Shrivastava, S. and Specht, F. R., Eds., ASM International, Materials Park, OH, 2002, pp. 76–83.
- [11] Felde, I., Réti, T., Sarmiento, G., Guerrero, M. and Grum, J., “Comparison Study of Numerical Methods Applied for Estimation of Heat Transfer Coefficient

- during Quenching”, *New Challenges in Heat Treatment and Surface Engineering*, Proceedings of the Conference in Honour of Prof. Božidar Liščić, Dubrovnik-Cavtat, Croatia, June 9–12, 2009, pp. 303–308.
- [12] Mattheij, R. M. M., Rienstra, S. W. and ten Thije Boonkkamp, J. H. M., *Partial Differential Equations: Modeling, Analysis, Computation*, SIAM, Philadelphia, 2005.
- [13] Brent, R. P., *Algorithms for Minimization without Derivatives*, Prentice–Hall, Englewood Cliffs, 1973.
- [14] Dierckx, P., *Curve and Surface Fitting with Splines*, Clarendon Press, Oxford, 1993.
- [15] Savitzky, A. and Golay, M. J. E., “Smoothing and Differentiation of Data by Simplified Least Squares Procedures”, *Anal. Chem.*, Vol. 36, 1964, pp. 1627–1639.
- [16] INCONEL alloy 600, Publication Number SMC–027, Special Metals Corporation, 2008.
- [17] Clark, J. and Tye, R., “Thermophysical Properties Reference Data for Some Key Engineering Alloys”, *High Temp.—High Press.*, Vol. 35/36, 2003/2007, pp. 1–14.
- [18] Akima, H., “A New Method of Interpolation and Smooth Curve Fitting Based on Local Procedures”, *J. Assoc. Comput. Mach.*, Vol. 17, No. 4, 1970, pp. 589–602.
- [19] de Boor, C., *A Practical Guide to Splines*, Rev. Ed., Springer, New York, 2001.
- [20] Liščić, B., Singer, S. and Beitz, H., “Dependence of the Heat Transfer Coefficient at Quenching on Diameter of Cylindrical Workpieces”, *J. ASTM Int.*, Vol. 8, No. 7, 2011.
- [21] Mitchell, A. R. and Griffiths, D. F., *The Finite Difference Method in Partial Differential Equations*, John Wiley & Sons Ltd., Chichester, 1980.